Transfer- and Fusion-Induced Fission of ^{238}U and ^{12}C : Experimental Observables

D. Ramos[1], C. Rodríguez-Tajes[2], M. Caamaño[1], F. Farget[2], L. Audouin[3], J. Benlliure[1], E. Casarejos[4], E. Clement[2], D. Cortina[1], O. Delaune[2], X. Derkx[5,*], A. Dijon[2], D. Doré[6], B. Fernández-Domínguez[1], G. de France[2], A. Heinz[7], B. Jacquot[2], A. Navin[2], C. Paradela[1], M. Rejmund[2], T. Roger[2], M.-D. Salsac[6], C. Schmitt[2]

(1) Dpto. Física de Partículas, USC, Santiago de Compostela, Spain. (2) GANIL, CEA/DMS - CNRS/IN2P3, Caen, France. (3) IPN Orsay, Université de Paris-Sud XI - CNRS/IN2P3, Orsay, France. (4) CIMA, Escuela Técnica Superior de Ingenieros Industriales, UVigo, Vigo, Spain. (5) LPC Caen, Université de Caen Basse-Normandie – ENSICAEN - CNRS/IN2P3, Caen, France. (6) CEA Saclay, DSM/IRFU/SPhN, Saclay, France. (7) Chalmes University of Technology, Göteborg, Sweden.

Fission at FUSTIPEN II, Caen, France

03/05/2016

Goals of Inverse kinematics

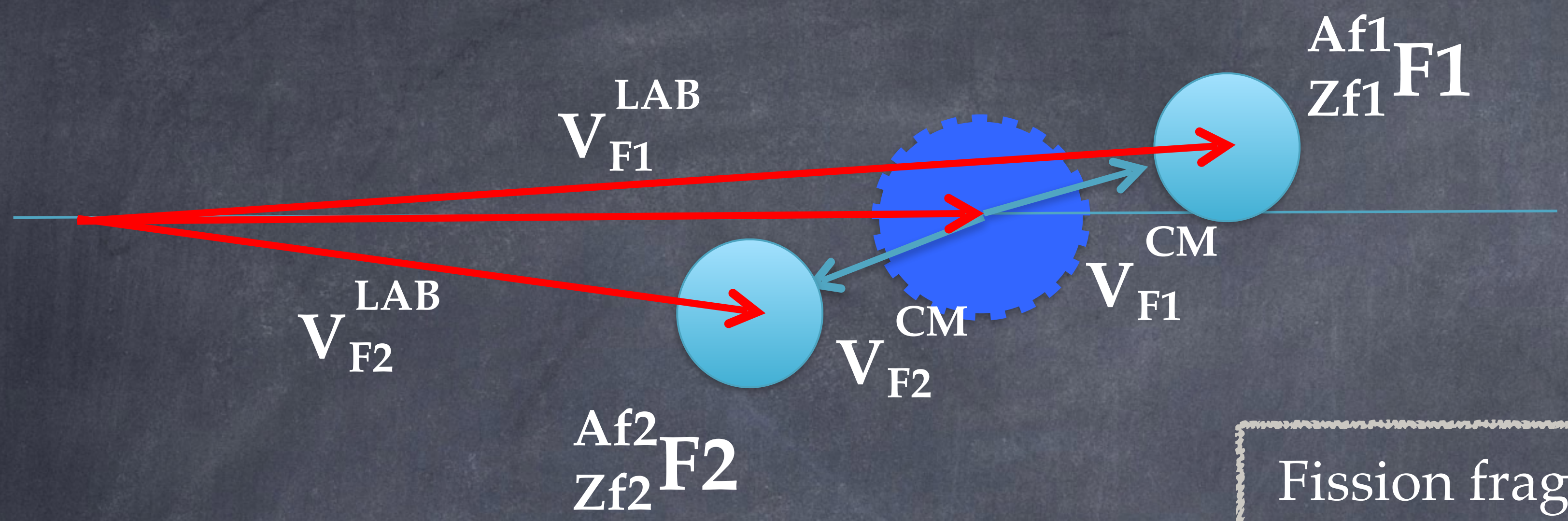

Fission fragment Z matrix identification

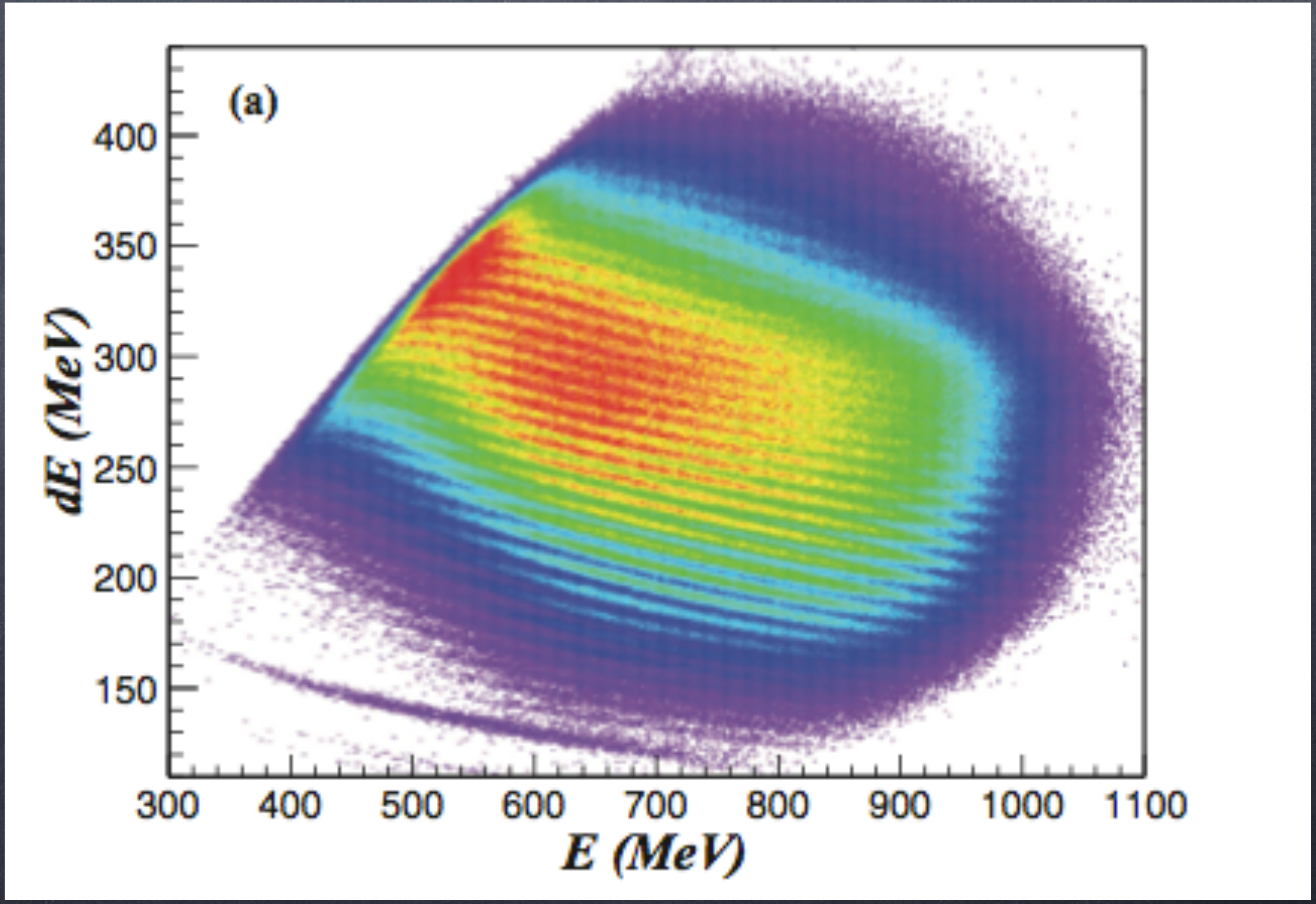

Kinematical boost increases the kinetic energy of the fission fragments providing **the capability of a direct identification**

Kinematical boost allows to keep a wide angular coverage in the CM frame when the size of the detectors is limited

Reaction Mechanism

$^{238}U + ^{12}C$ @ 6.14 AMeV

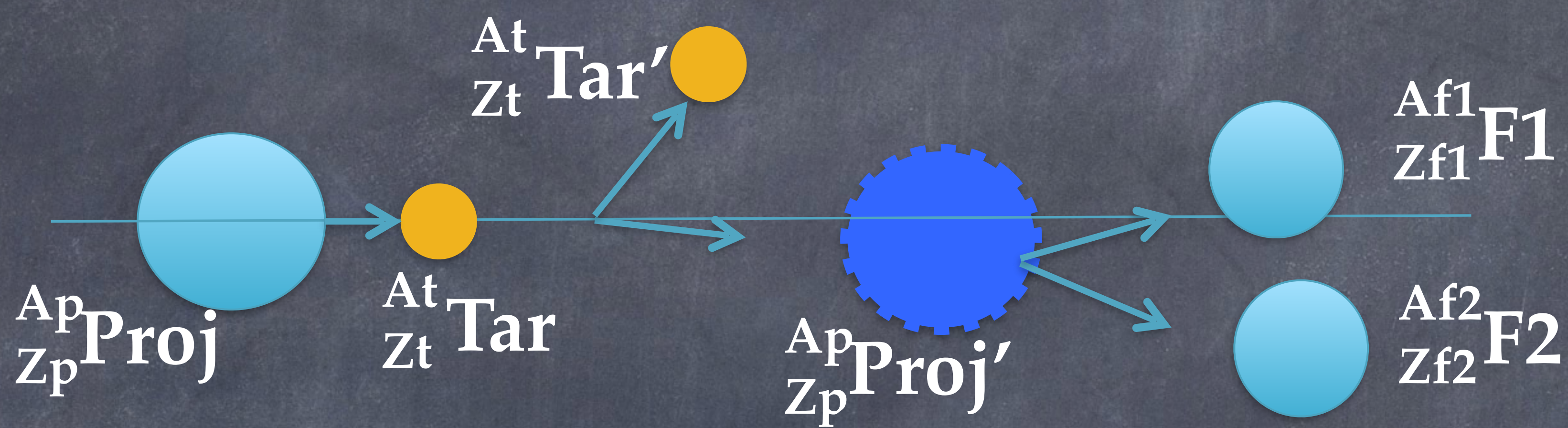

Fissioning Systems

242 Cf	243 Cf	244 Cf	245 Cf	246 Cf	247 Cf	248 Cf	249 Cf	250 Cf	251 Cf	252 Cf
241 Bk	242 Bk	243 Bk	244 Bk	245 Bk	246 Bk	247 Bk	248 Bk	249 Bk	250 Bk	251 Bk
240 Cm	241 Cm	242 Cm	243 Cm	244 Cm	245 Cm	246 Cm	247 Cm	248 Cm	249 Cm	250 Cm
239 Am	240 Am	241 Am	242 Am	243 Am	244 Am	245 Am	246 Am	247 Am	248 Am	249 Am
238 Pu	239 Pu	240 Pu	241 Pu	242 Pu	243 Pu	244 Pu	245 Pu	246 Pu	247 Pu	
237 Np	238 Np	239 Np	240 Np	241 Np	242 Np	243 Np	244 Np			
236 U	237 U	238 U	239 U	240 U	241 U	242 U				

Fissioning systems difficult to produce by another mechanism

10% above Coulomb barrier

Transfer-Fission:

10 n-rich actinides produced with a distribution of E_X below 30 MeV

Fusion-Fission:

production of ^{250}Cf with $E_X = 45$ MeV 10 times more likely than any transfer channel

Transfer Reaction and Excitation Energy

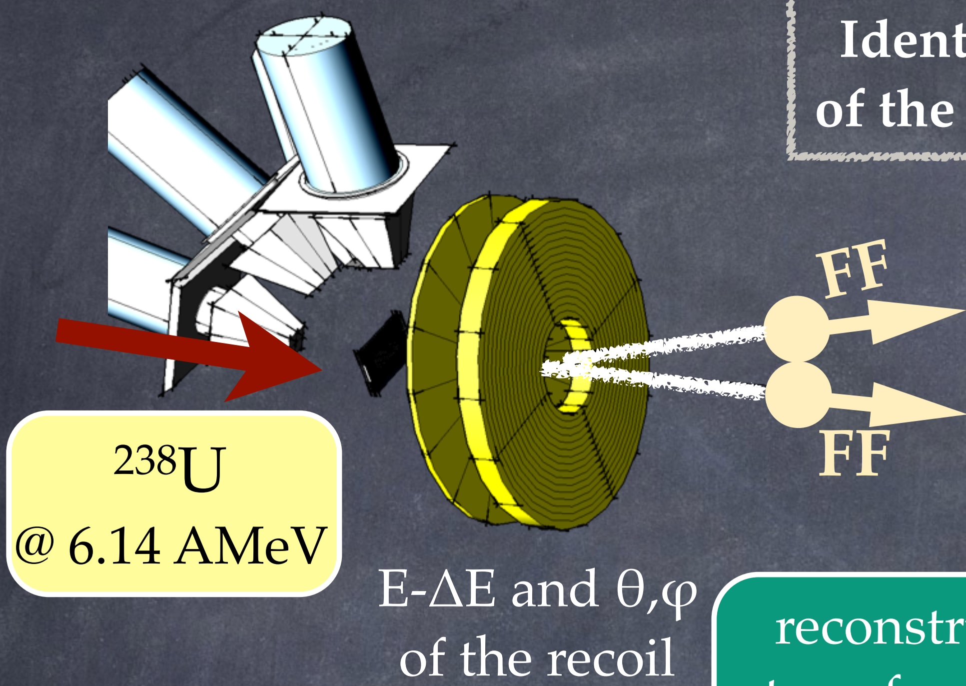

reconstruction of the transfer reaction & E*

Identification Matrix of the target-like recoil

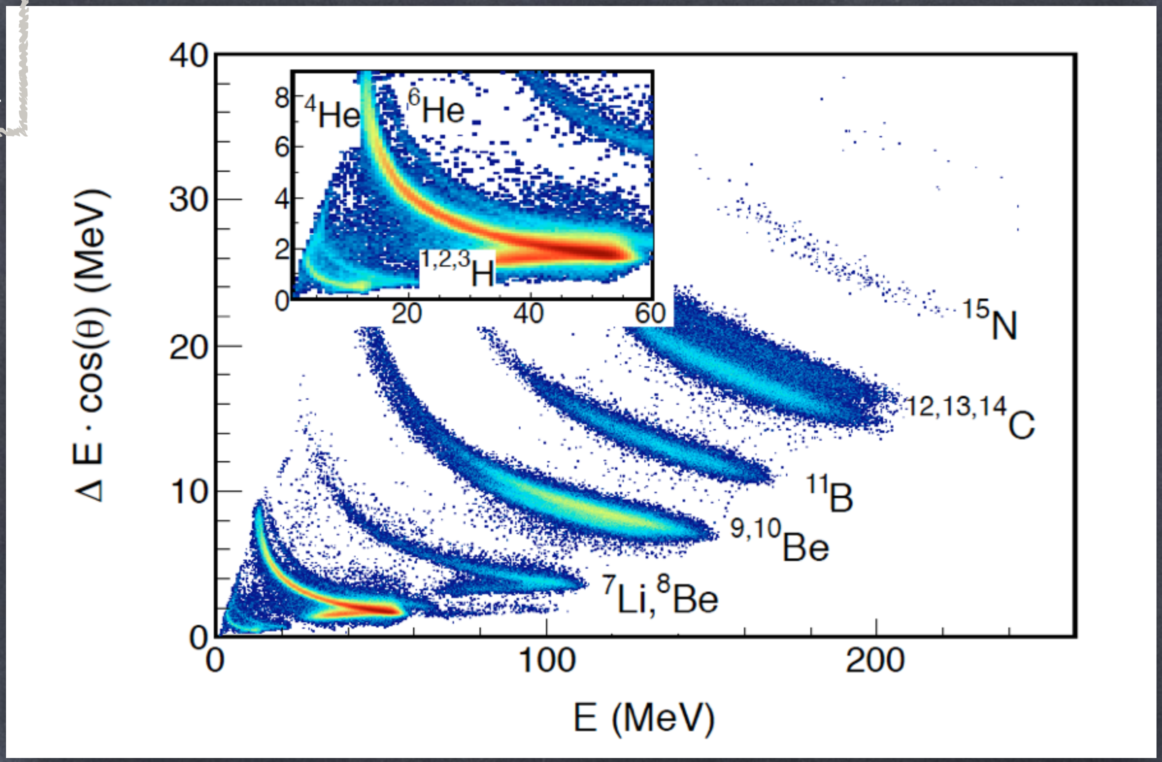

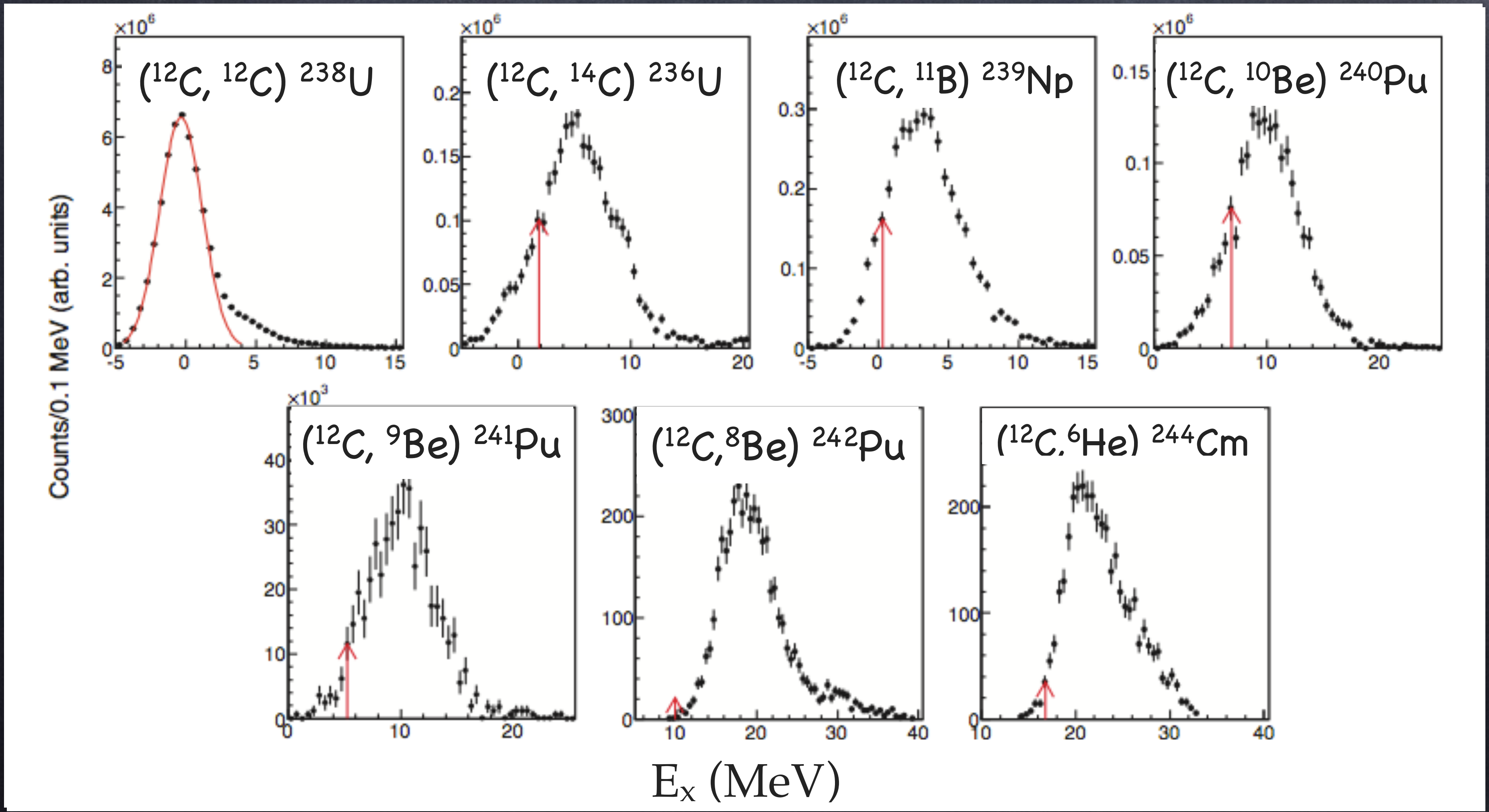

Distribution of E_x for the different fissioning systems from reconstruction of the binary reaction

Higher E_x for higher number of transferred nucleons

E_x ~ 8 MeV is comparable with fast-neutron fission

C. Rodriguez-Tajes et *al*., PRC (2014) 024614

Excitation of Target-like Recoil

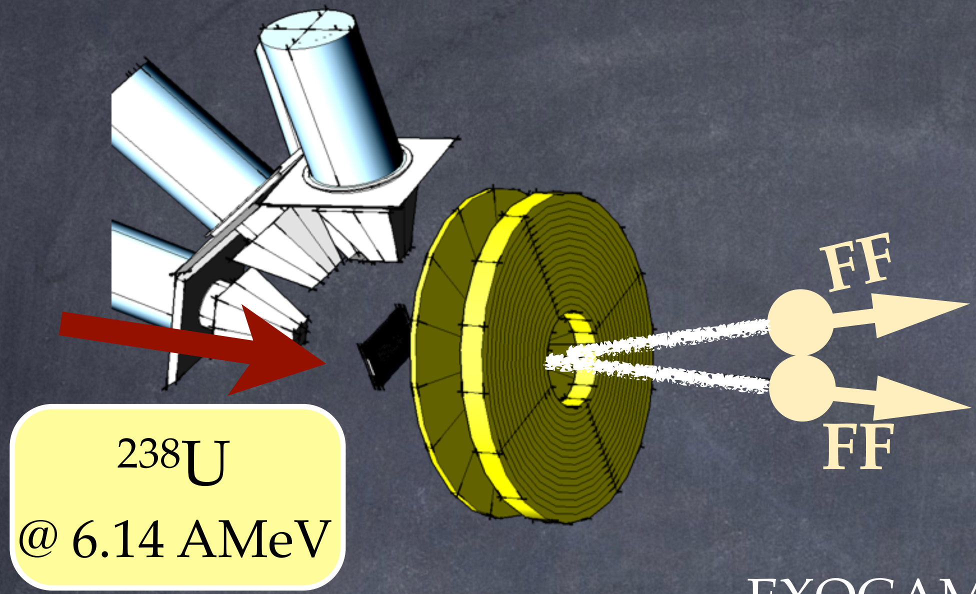

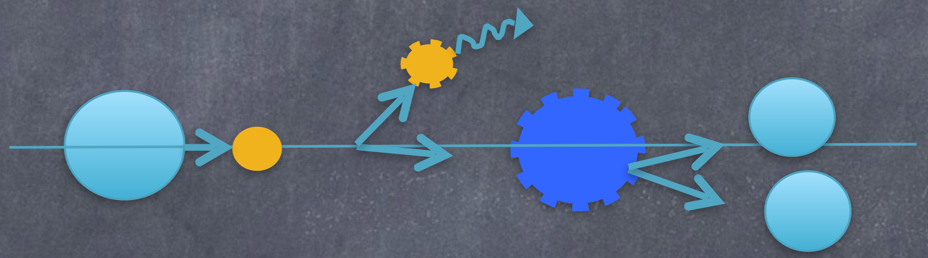

EXOGAM detector allow us to evaluate the excitation probability of the target-like nuclei

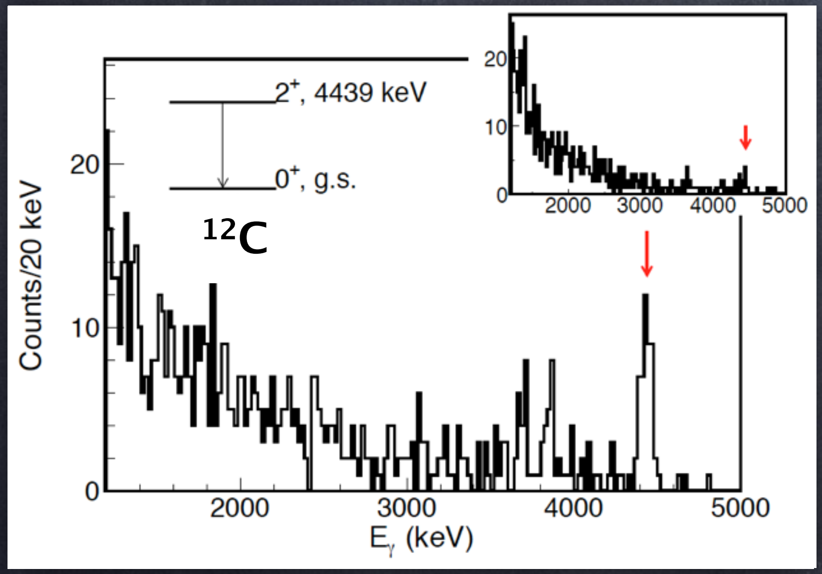

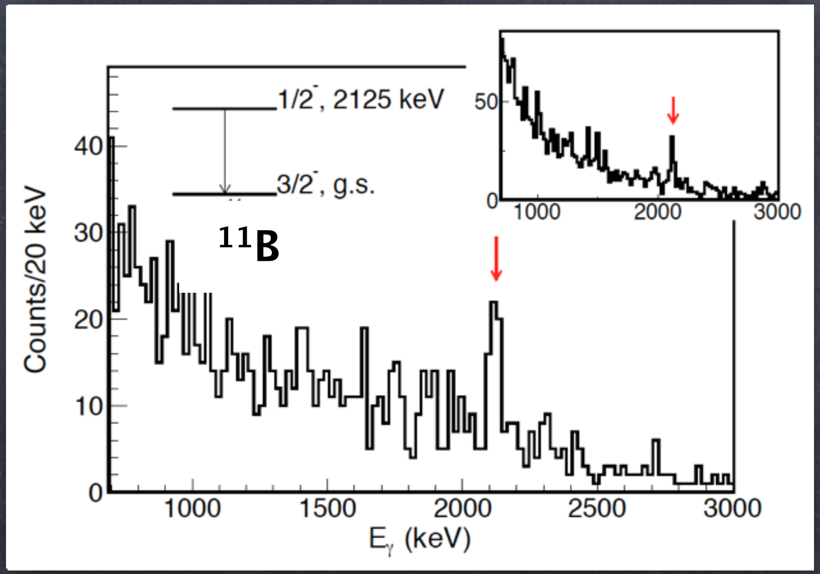

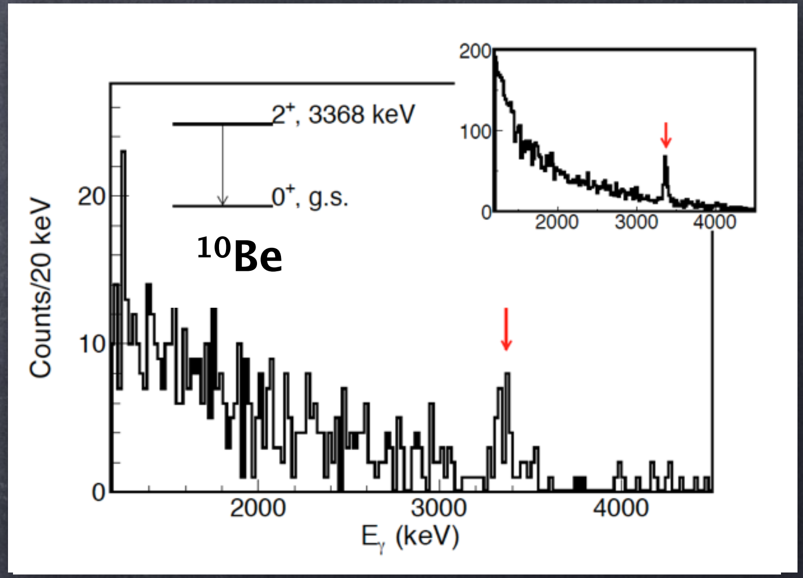

γ-rays measurements show excited states in ^{12}C, ^{11}B and ^{10}Be **in coincidence with fission with P$_\gamma$ = 0.12-0.14**

C. Rodriguez-Tajes et *al.*, PRC (2014) 024614

Fission Fragments Detection

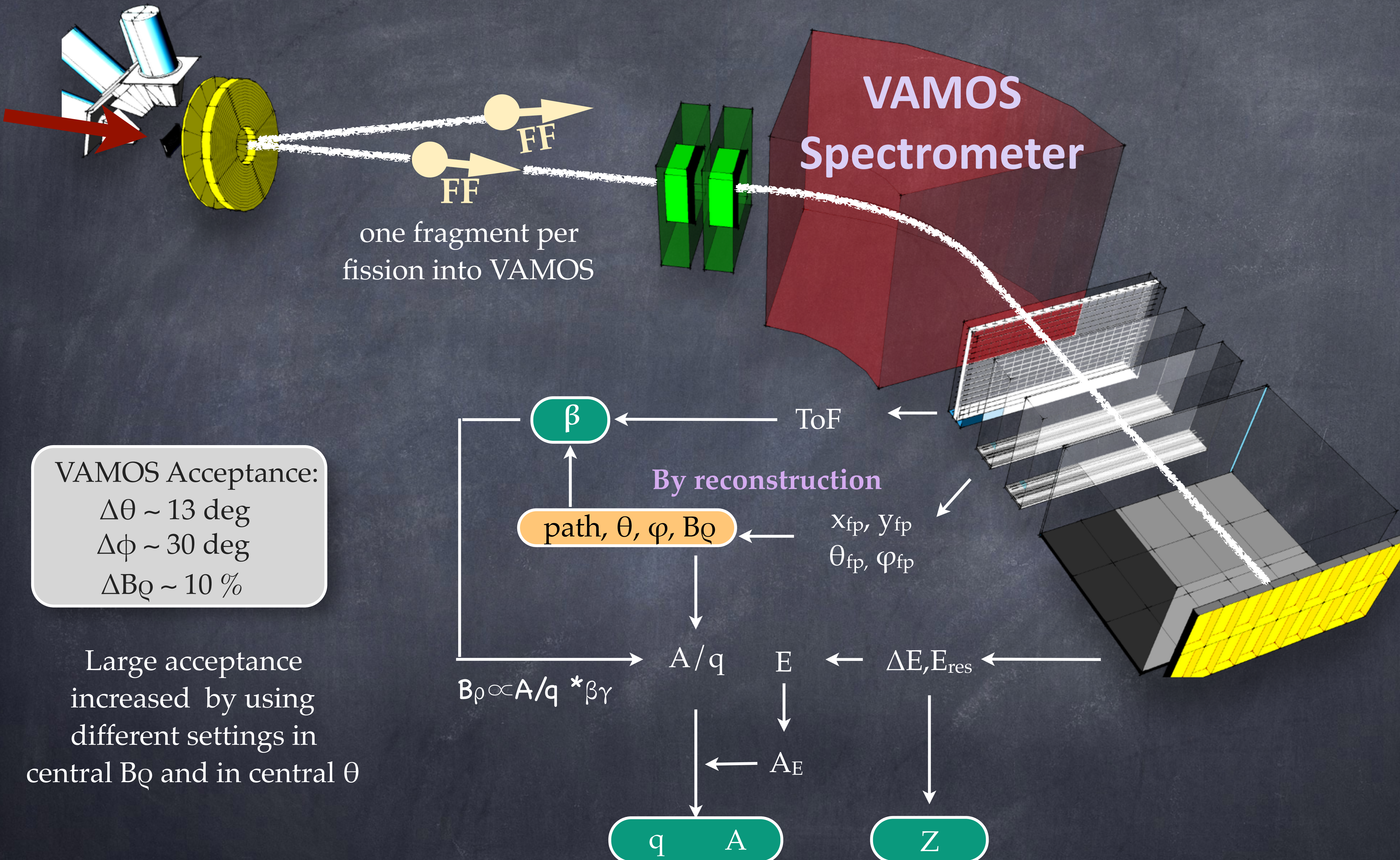

VAMOS Acceptance:
$\Delta\theta \sim 13$ deg
$\Delta\phi \sim 30$ deg
$\Delta B\rho \sim 10$ %

Large acceptance increased by using different settings in central Bρ and in central θ

M. Rejmund et al., NIM A 646 (2011) 184
S. Pullanhiotan et al., NIM A 593 (2008) 343

Fission Fragments Identification

Mass Identification

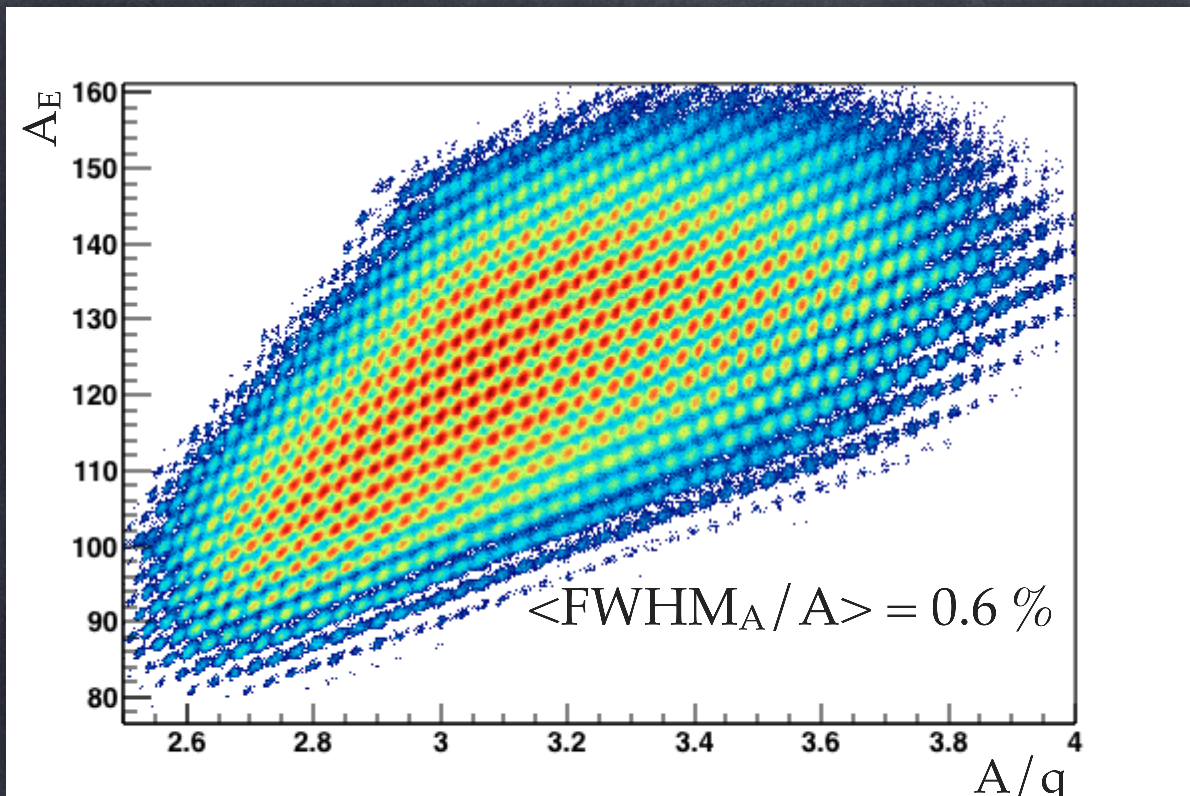

Nuclear Charge Identification

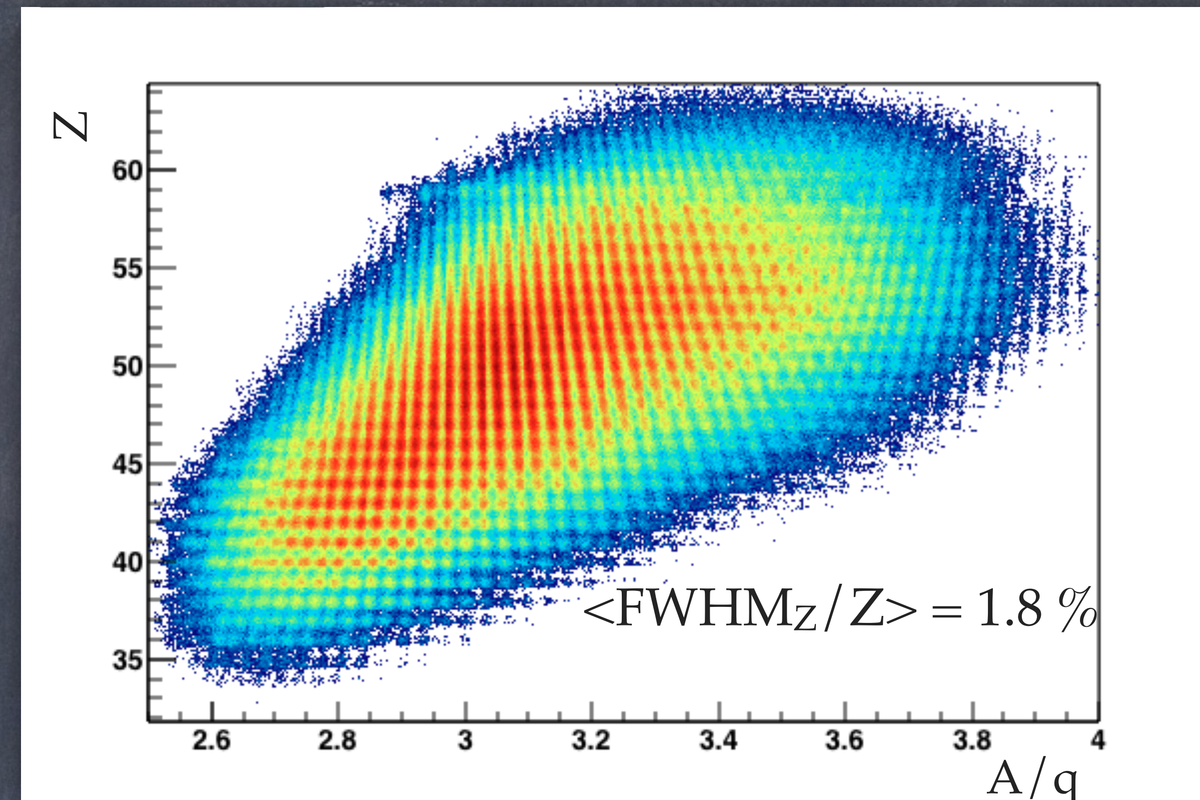

A/q provides the q separation and contributes to a better A resolution

More than 300 isotopes identified

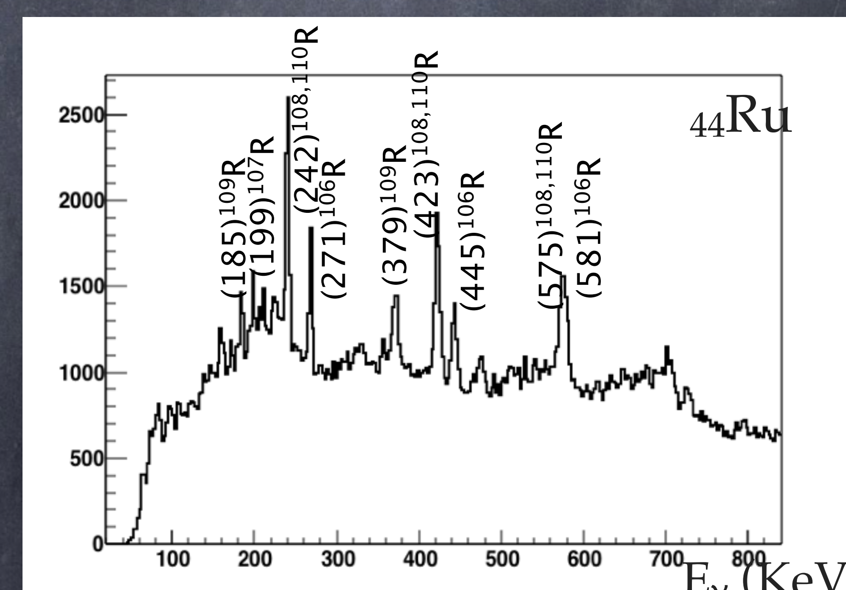

γ-rays in coincidence with fission fragments provide a cross check for the Z and A identification

A. Shrivastava et al. PRC 80 (2009) 051305

Transmission through VAMOS

4 settings of VAMOS covers different range of Bρ -Θ

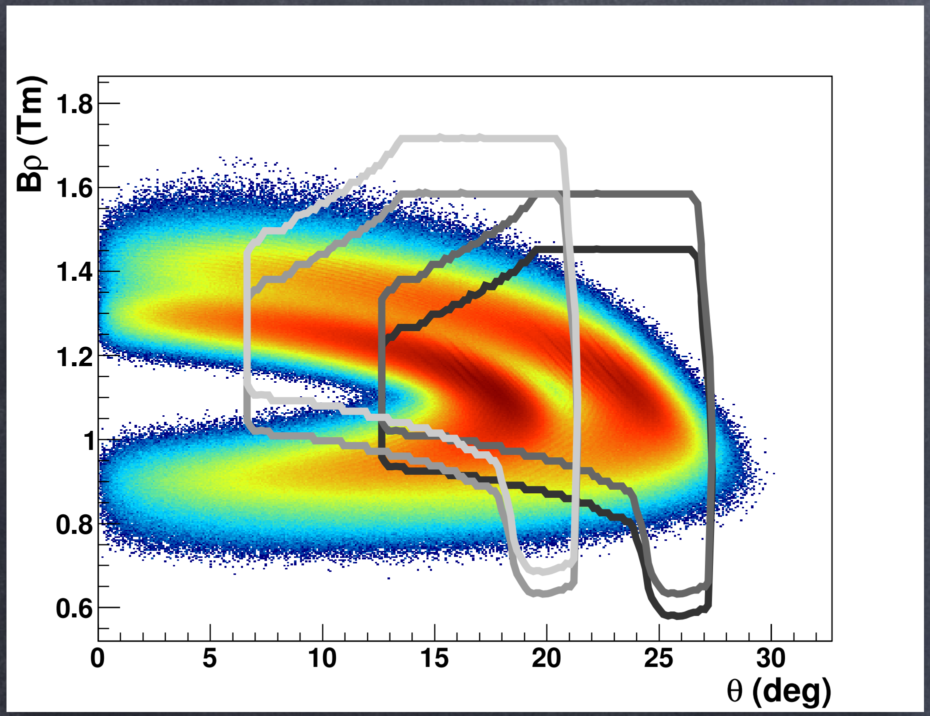

The transmission limits the angular range

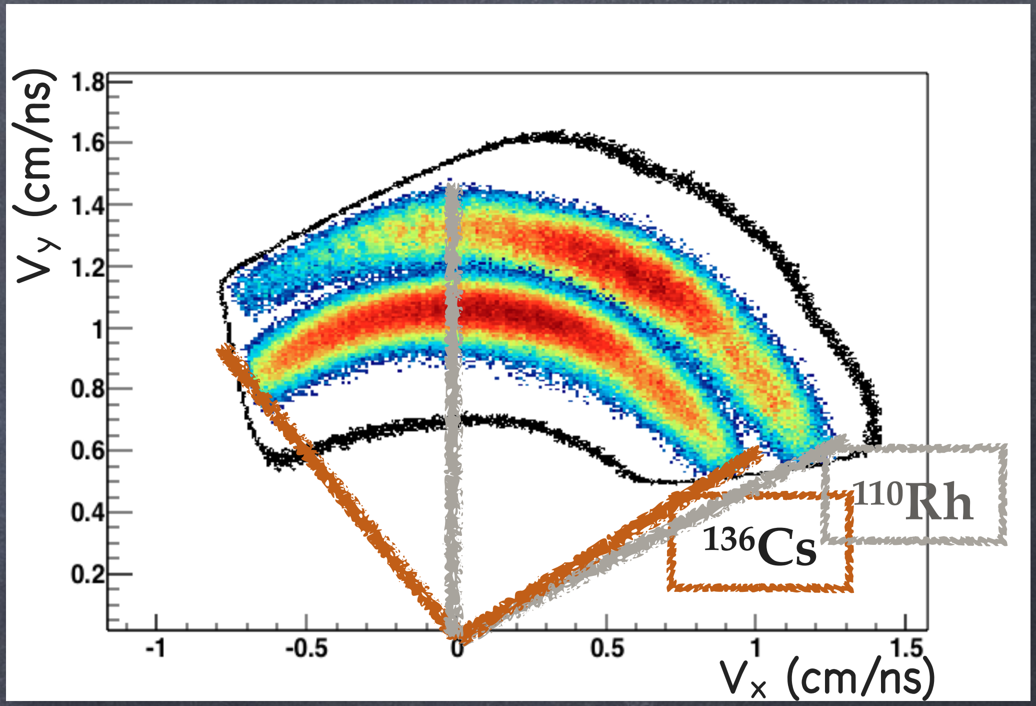

The angular coverage is larger for higher fission fragments

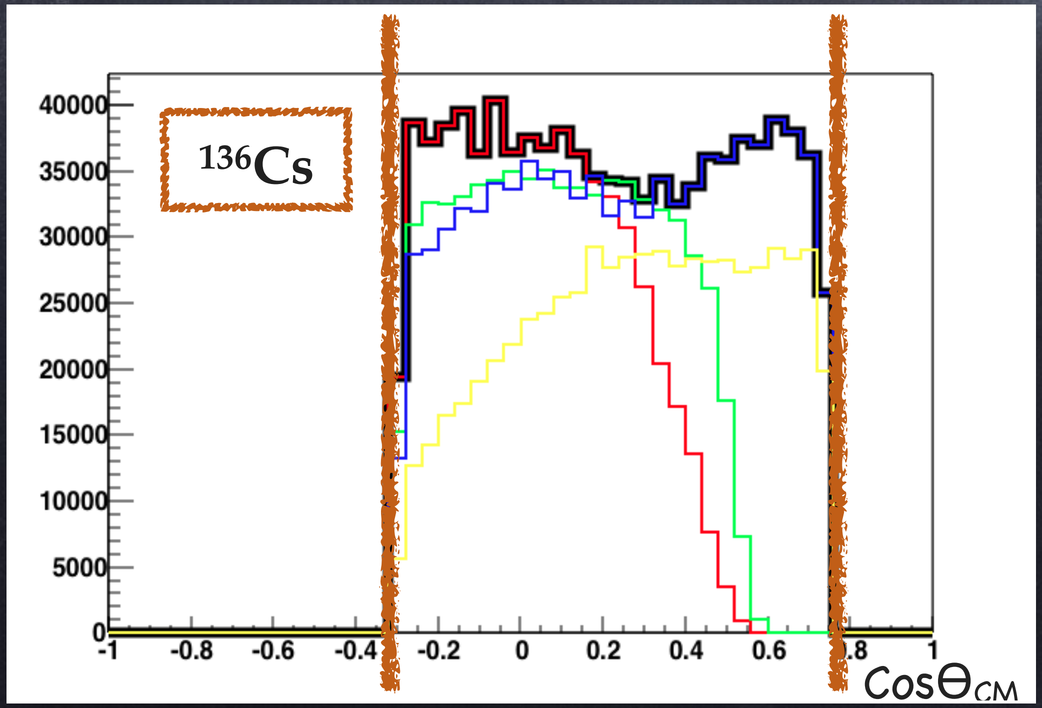

Beam normalization for different settings is required

Fission Yields Calculation

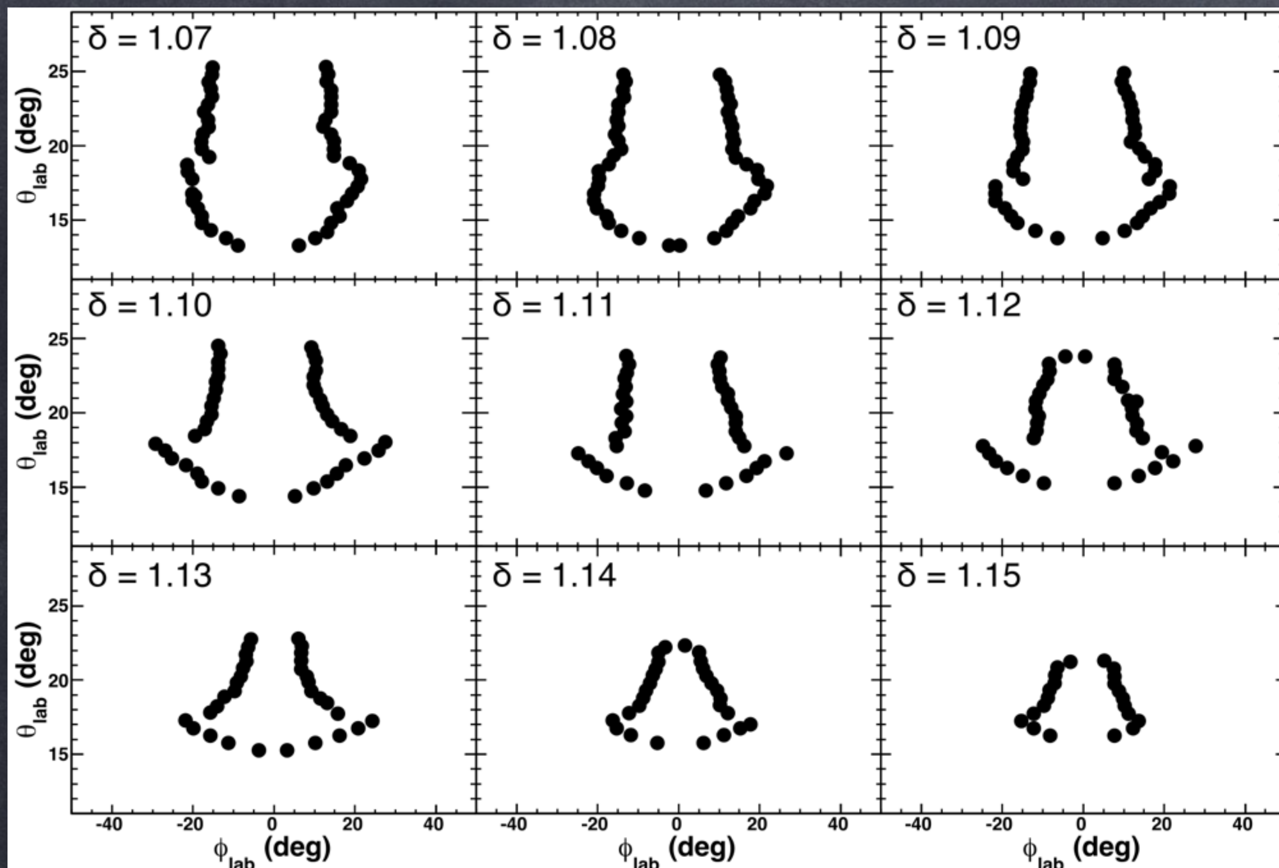

$$I(Z,A,q) = N(Z,A,q)\frac{2\pi}{Range_{\phi}(\delta,\theta)}$$

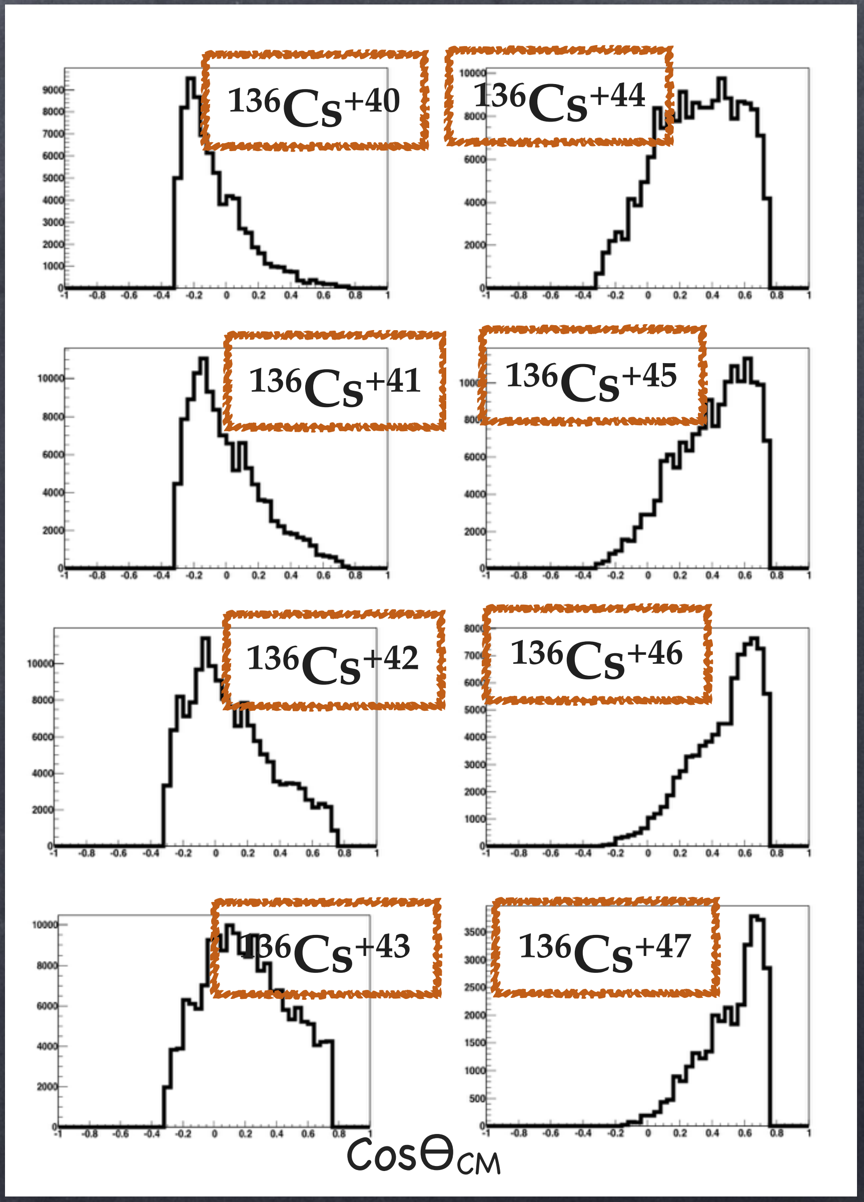

We need to recover all the charge states per isotope and compensate the acceptance in the azimuthal and polar angles

$$I(Z,A) = \sum_q I(Z,A,q)$$

$$Y(Z,A) = I(Z,A)\frac{2}{Range(Z,A)}$$

Isotopic Fission-Fragment Distribution

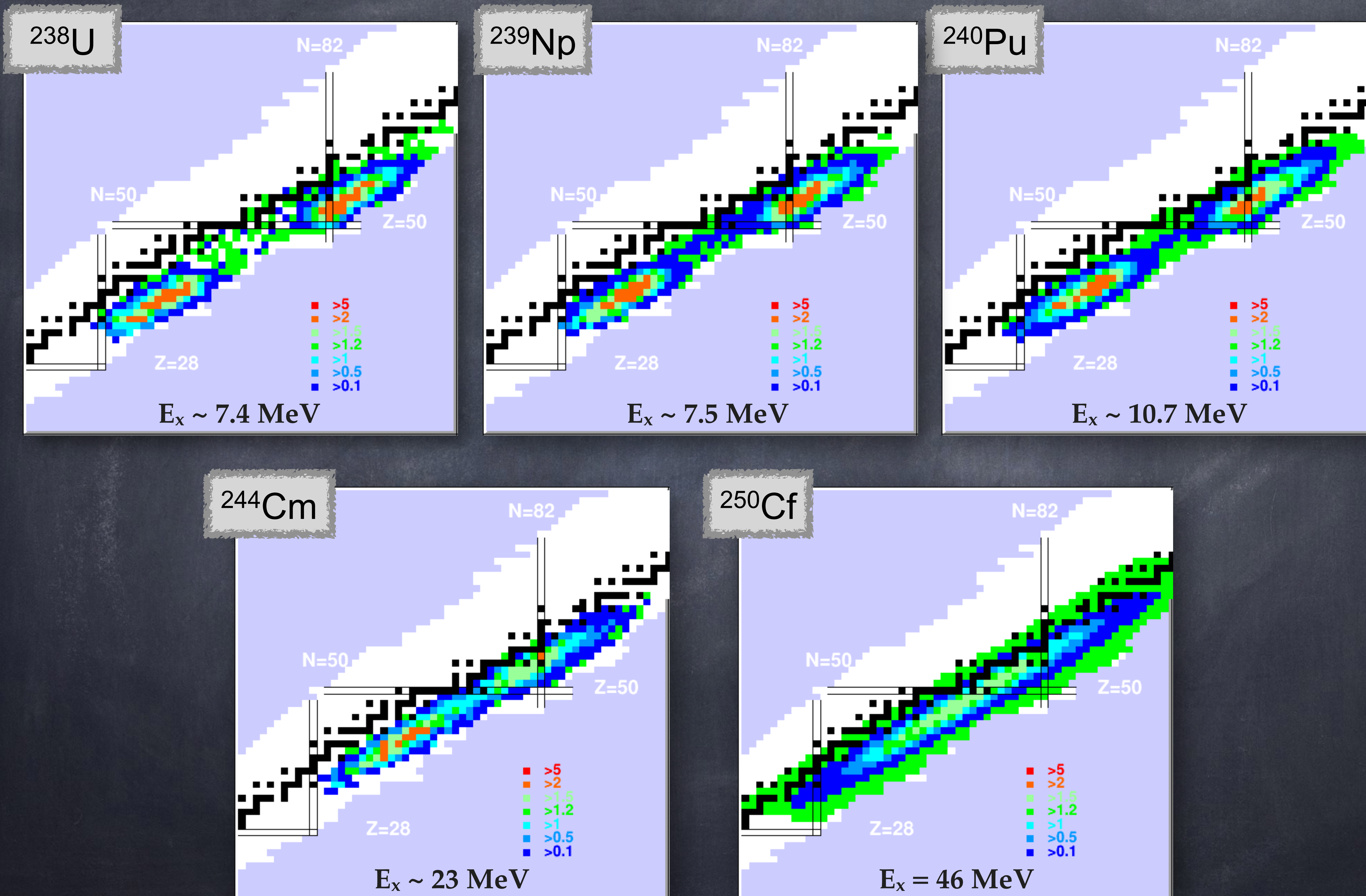

Fission Yields

Mass-yields and Z-yields distribution of 5 different fissioning systems, most of them exotic nuclei

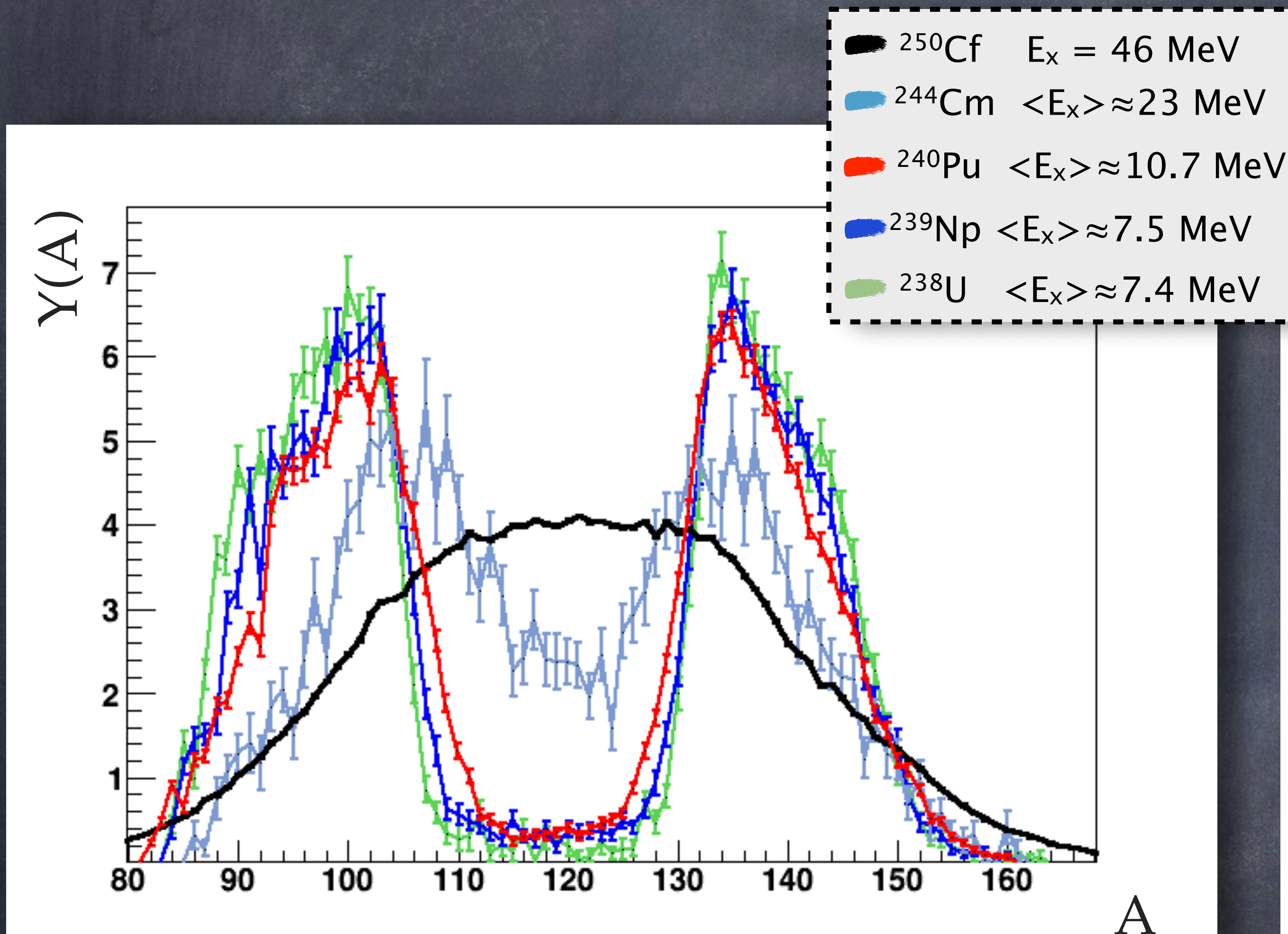

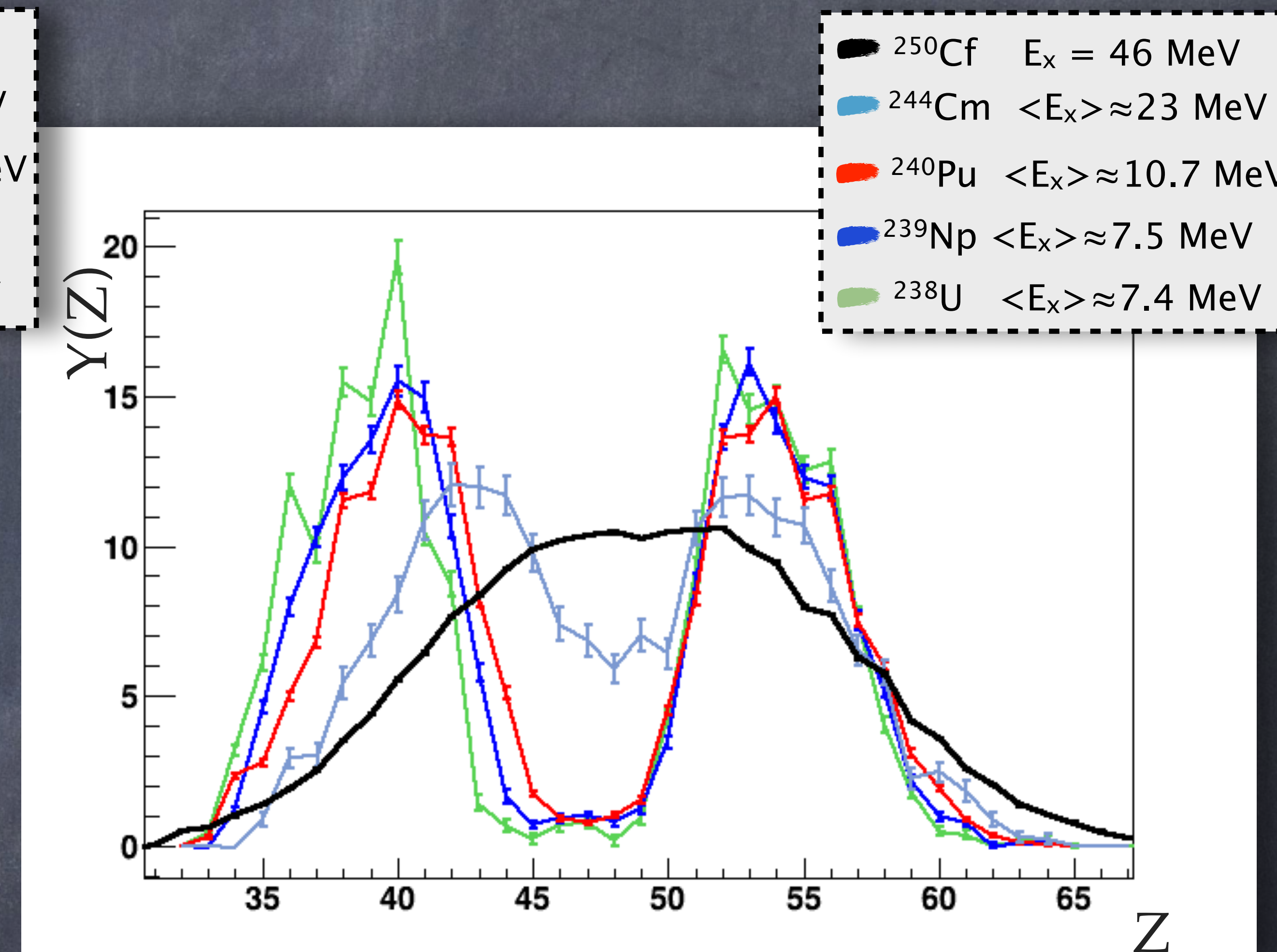

New complete measurements, difficult to produce by n-capture

Measurements of fragment distributions of ^{239}Np is scarce ($T_{1/2}$ (^{238}Np) = 2.1 d)

There is no direct measurements of fragment distributions of ^{244}Cm

The contribution of the symmetric mode disappears for the systems at low excitation energy

The shift in Z of the light fragments with the atomic number of the fissioning system reflects the stabilization of the heavy group

Fission Yields

^{238}U $\langle E_x \rangle \approx 7.4$ MeV

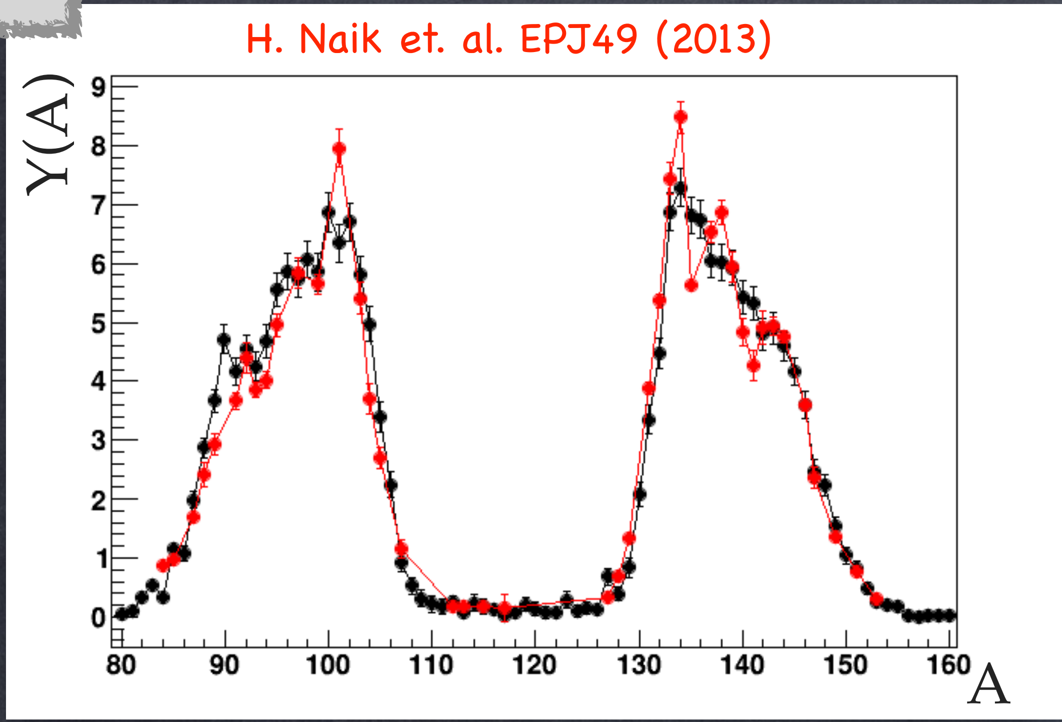

Bremsstrahlung γ-induced fission Ex~9 MeV

^{239}Np $\langle E_x \rangle \approx 7.5$ MeV

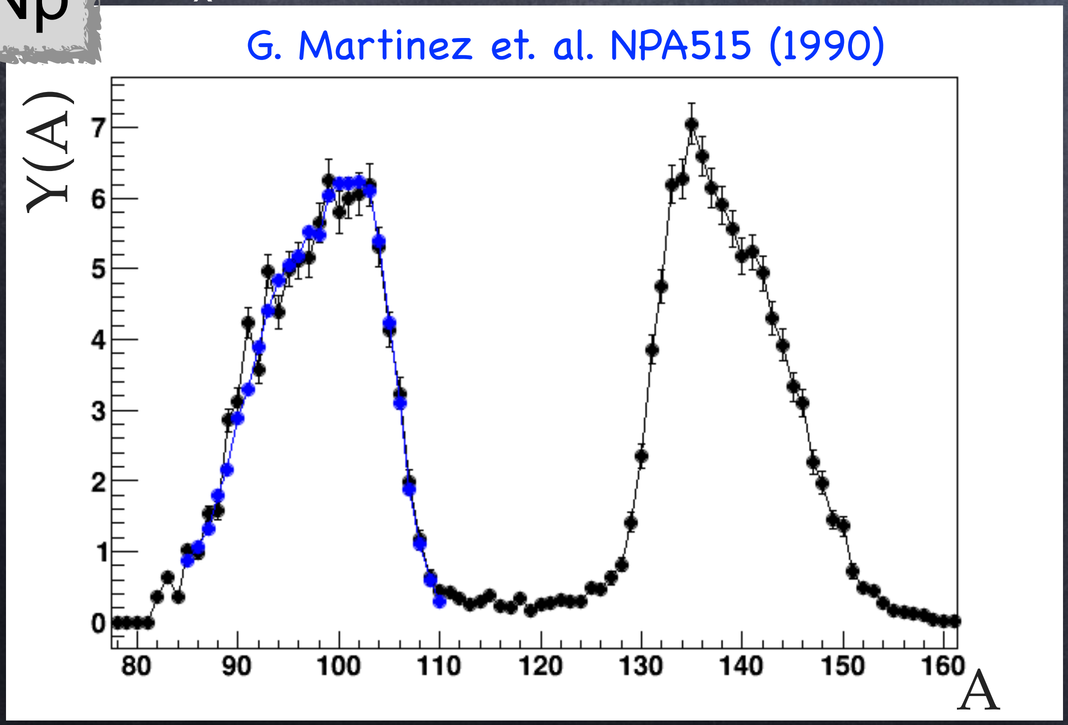

^{237}Np(2n$_{th}$, f) Ex~6.2 MeV

^{240}Pu $\langle E_x \rangle \approx 10.7$ MeV

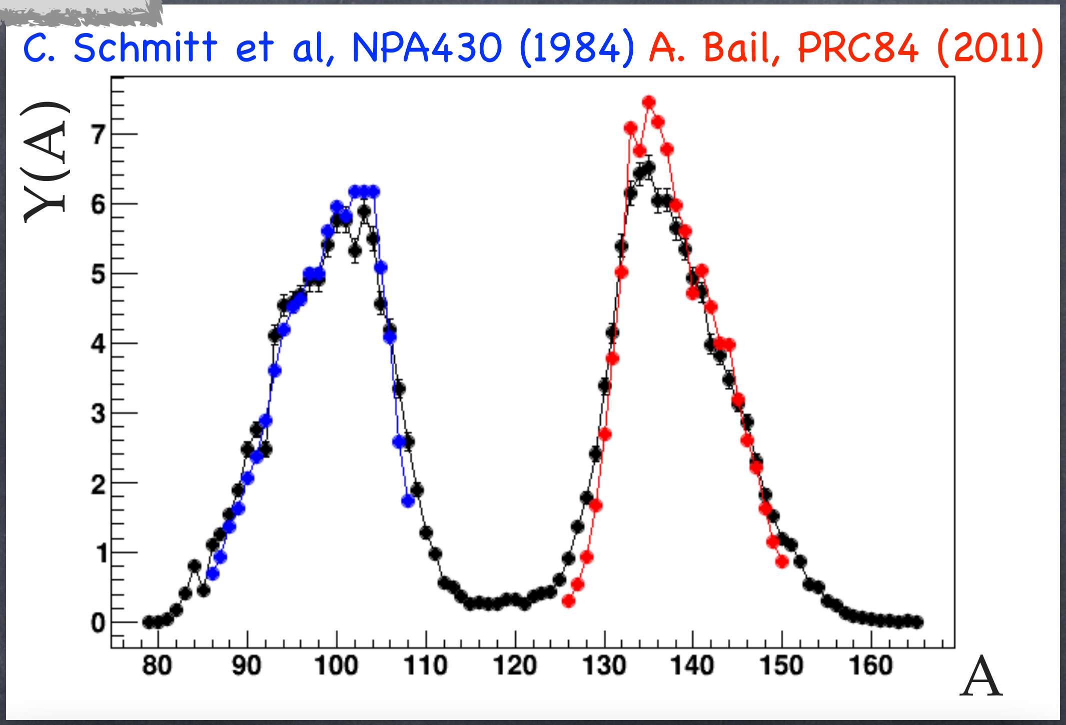

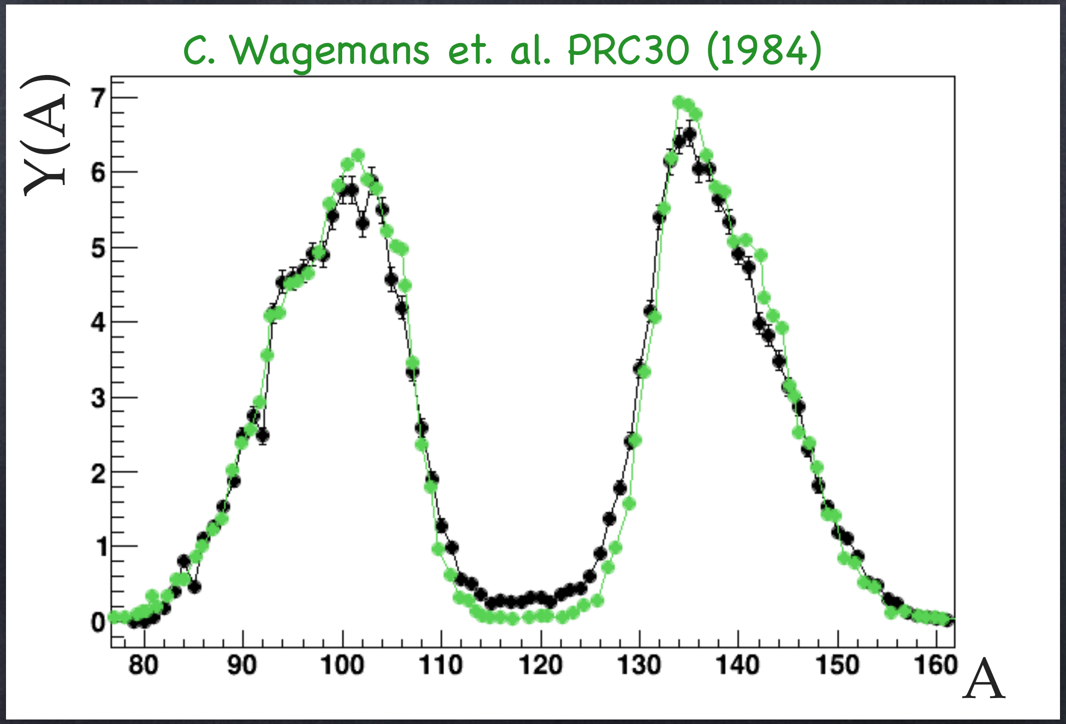

^{239}Pu(n$_{th}$, f) Ex~6.5 MeV

Neutron Excess

Evolution of the polarization with the E_x and the **fissioning system**

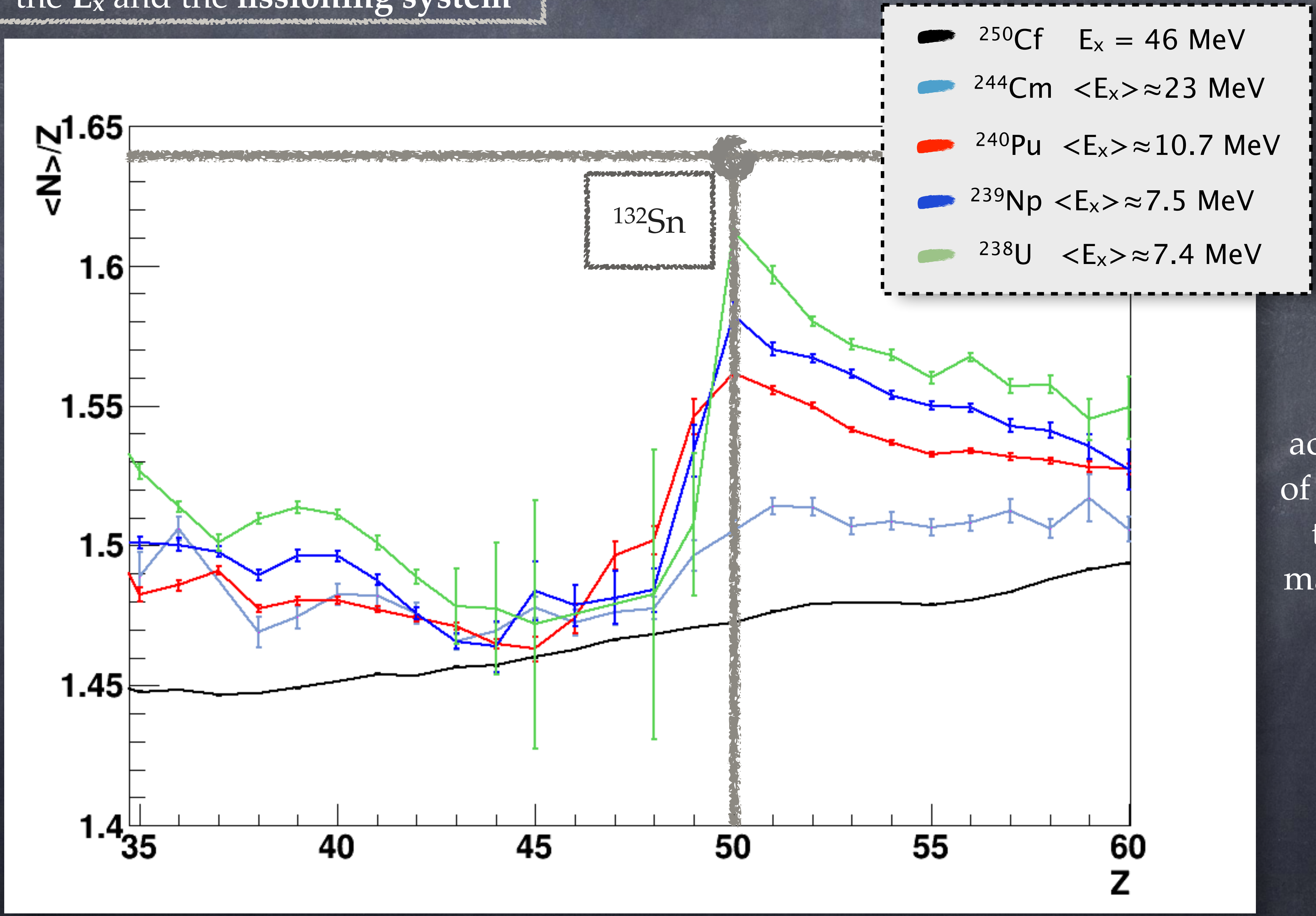

Clear accumulation of N driven by the double magic nucleus ^{132}Sn

Charge Polarization present in all the systems

Evolution with Excitation Energy

^{240}Pu

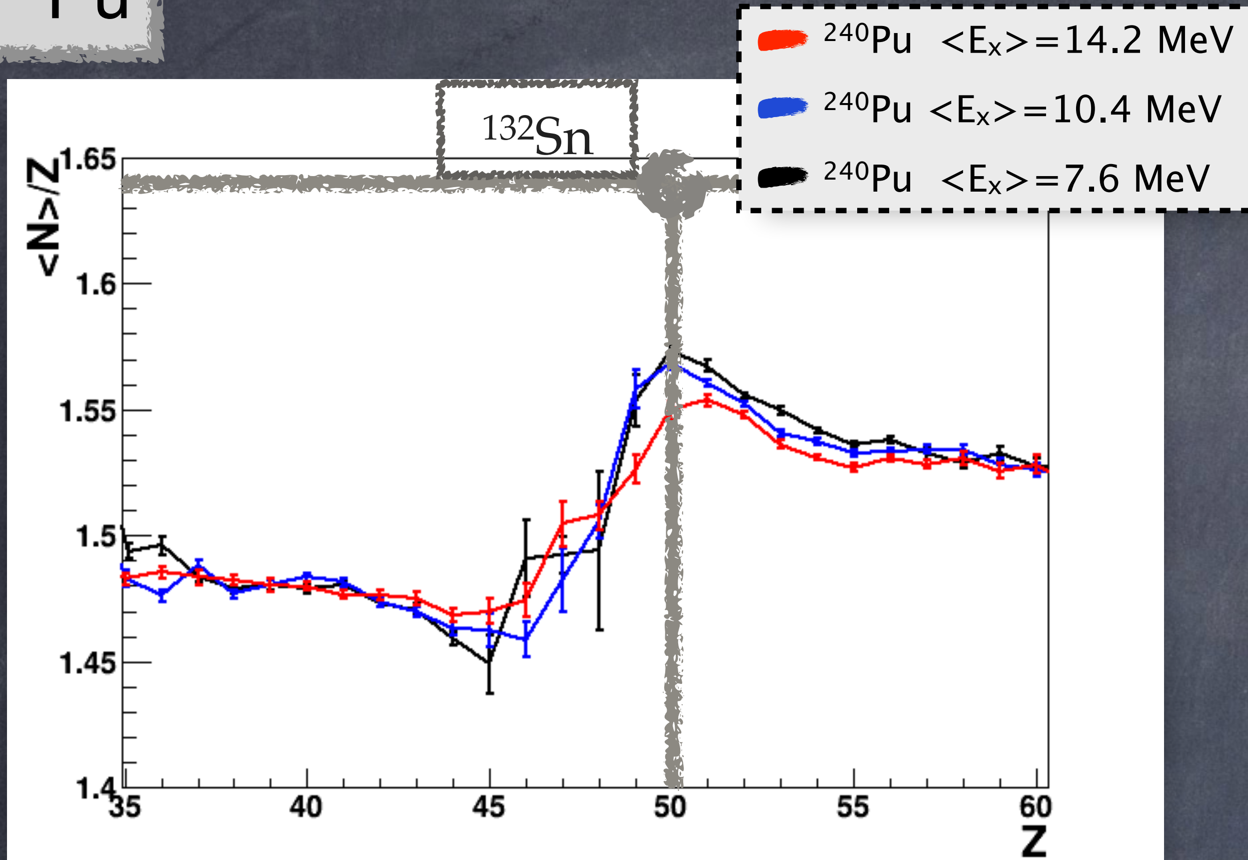

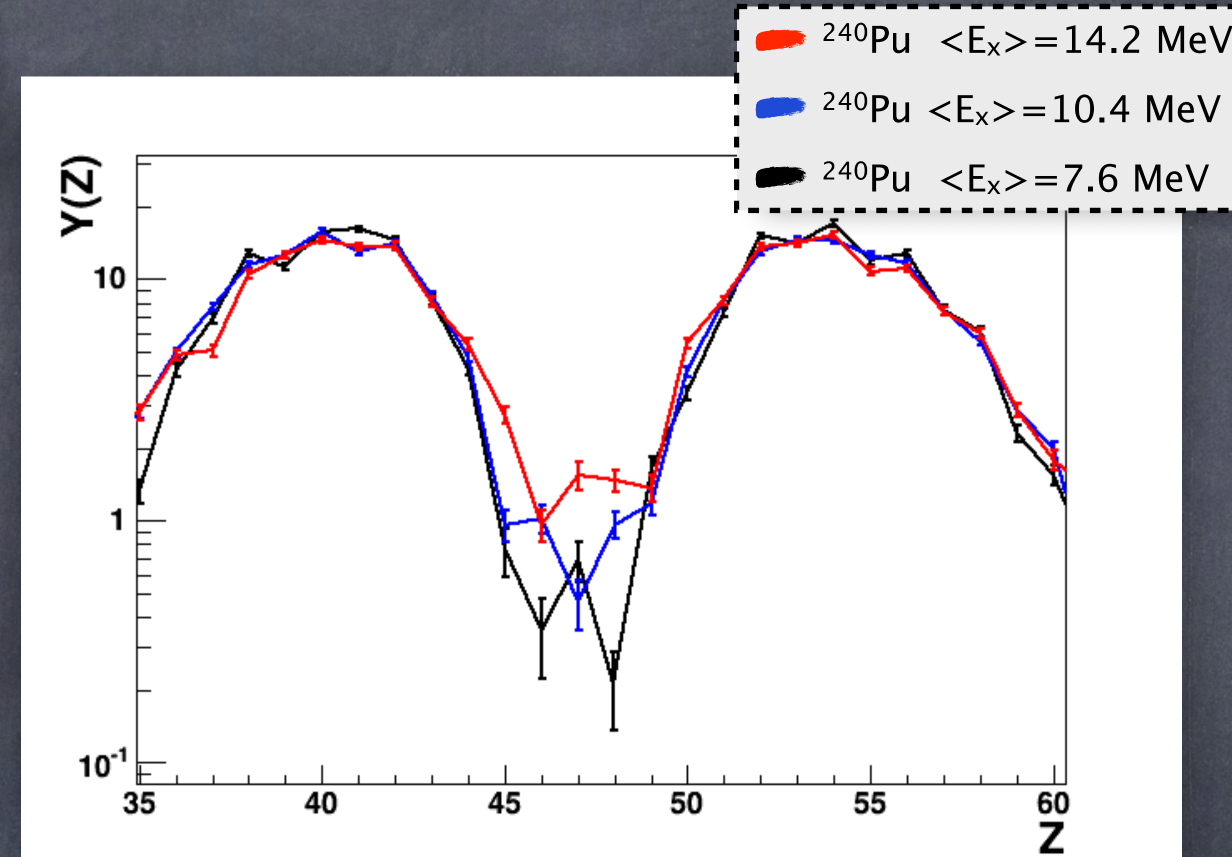

The $\langle N \rangle / Z$ ratio gets reduced around $Z \approx 50$ by increasing E_x, signature of a closed shell which effect is smaller for higher E_x.

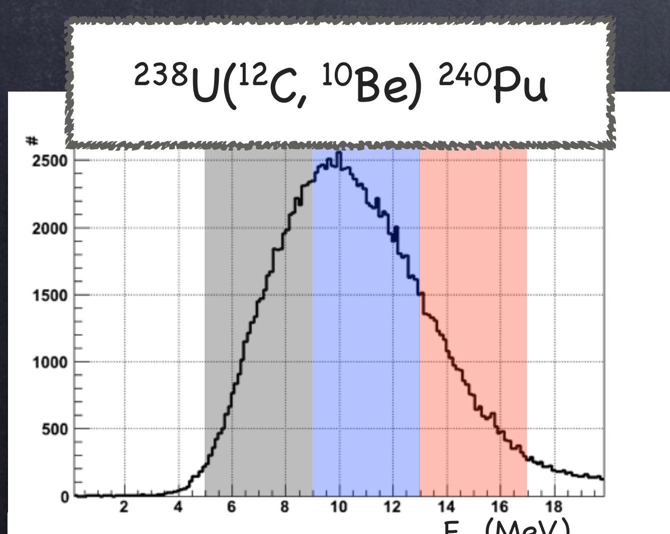

3 different regions of E_x were selected

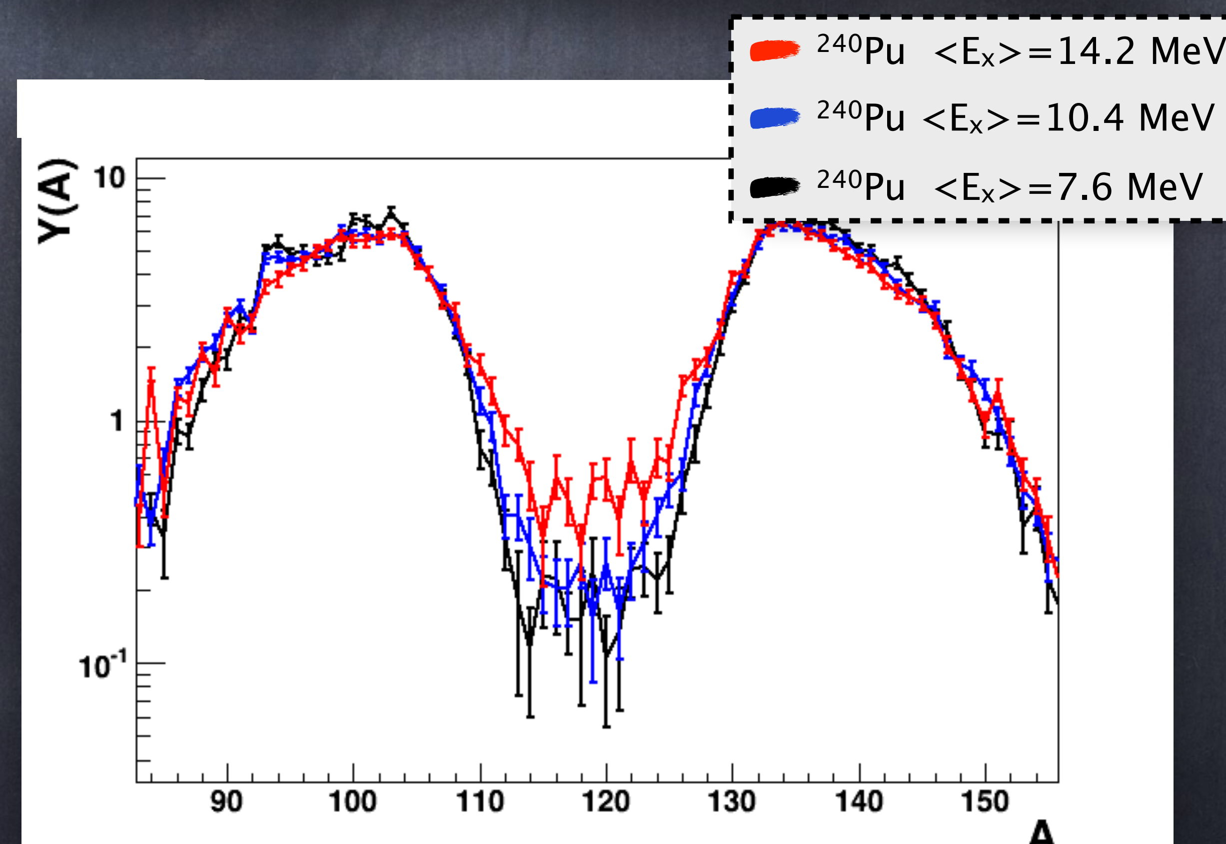

Total Kinetic Energy

PRELIMINARY

^{240}Pu

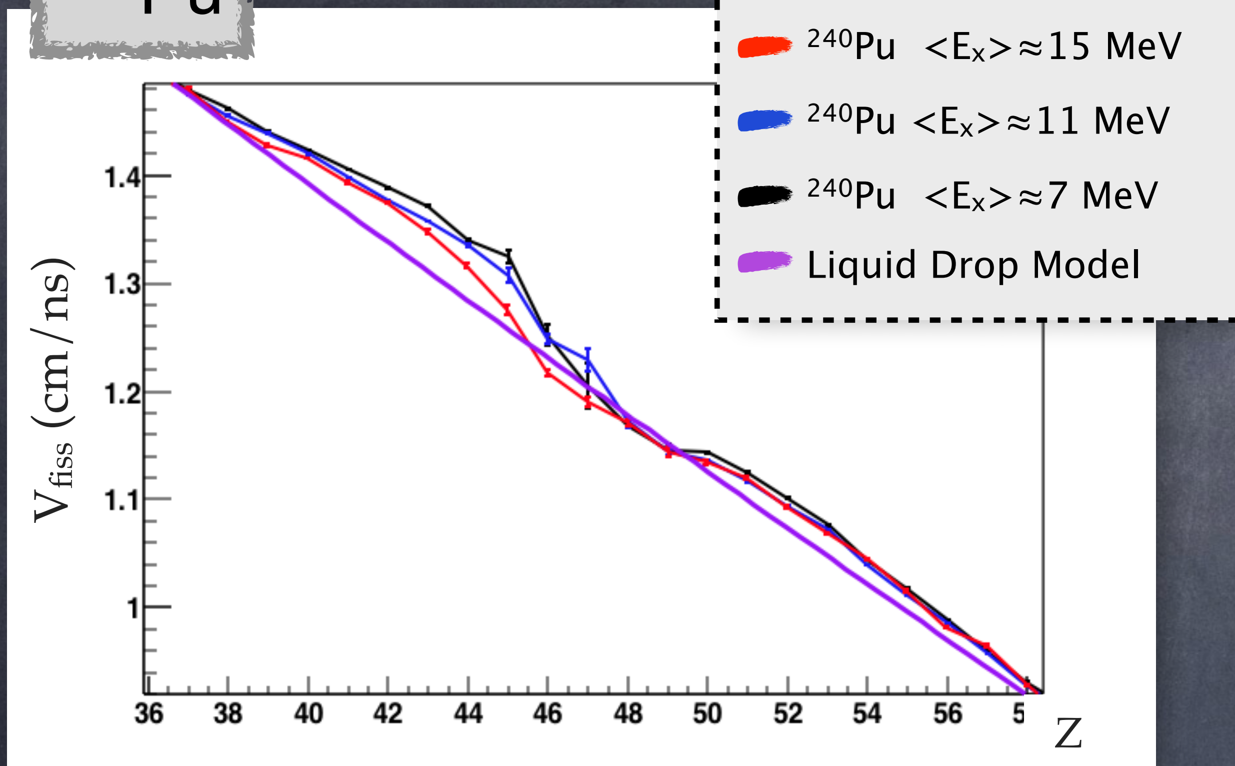

Mean value of the velocity of ff as a function of Z

In the asymmetric region, the light fragment is emitted with a higher velocity compared with the LDM

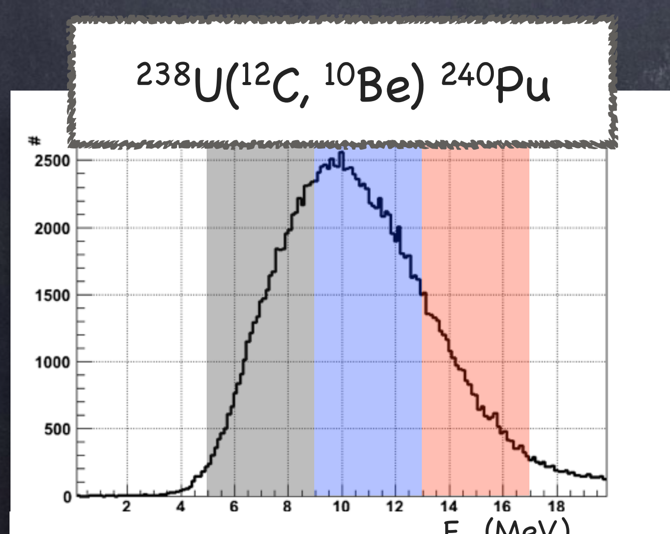

$$TKE = u\cdot < A >_Z \cdot(< \gamma >_Z -1) +$$
$$u\cdot < A >_{Z_{Act}-Z} \cdot(< \gamma >_{Z_{Act}-Z} -1)$$

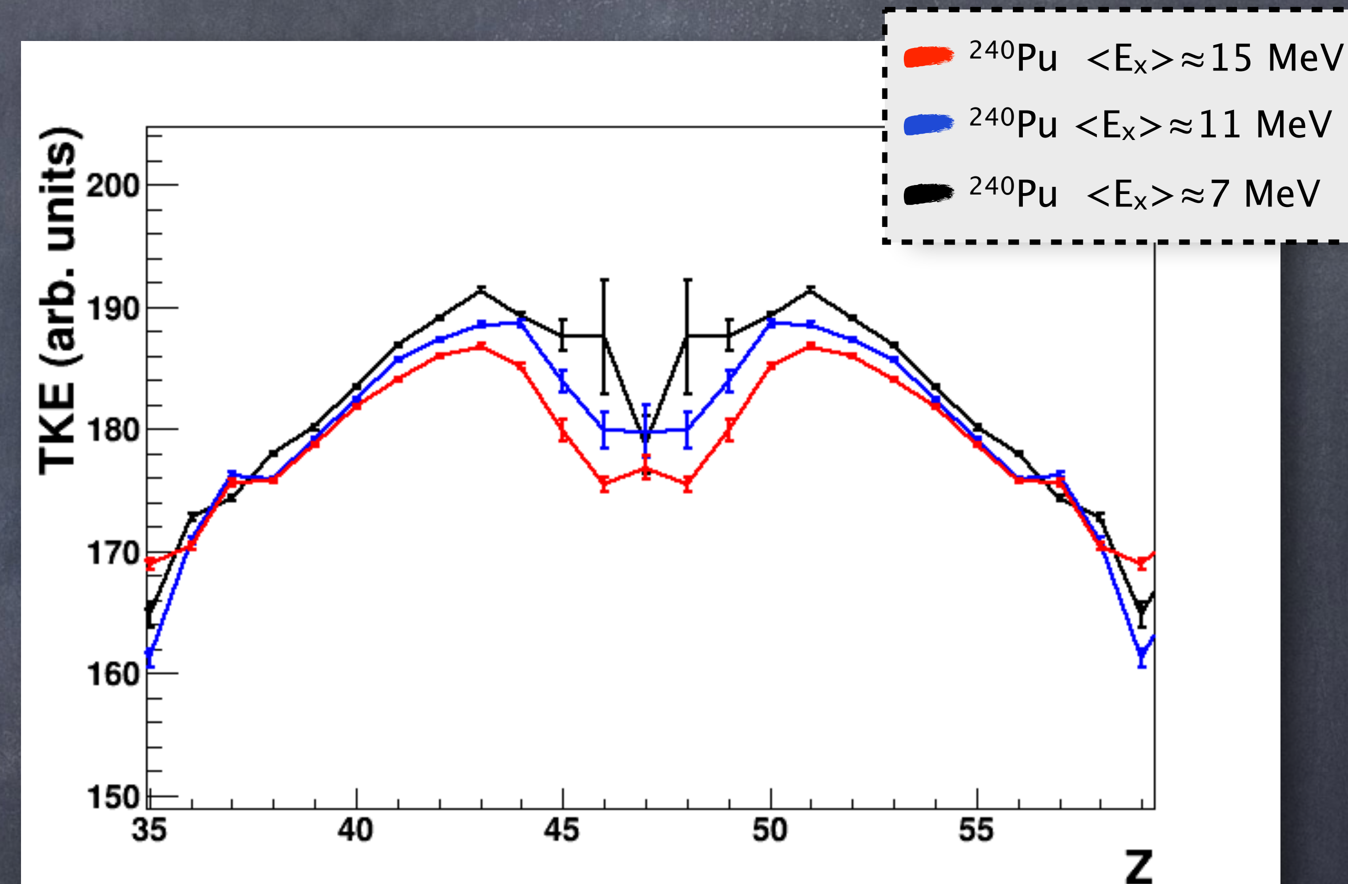

TKE values decrease with higher E_x
The distance between both fragments at the scission point is larger with higher E_x

Fission Modes

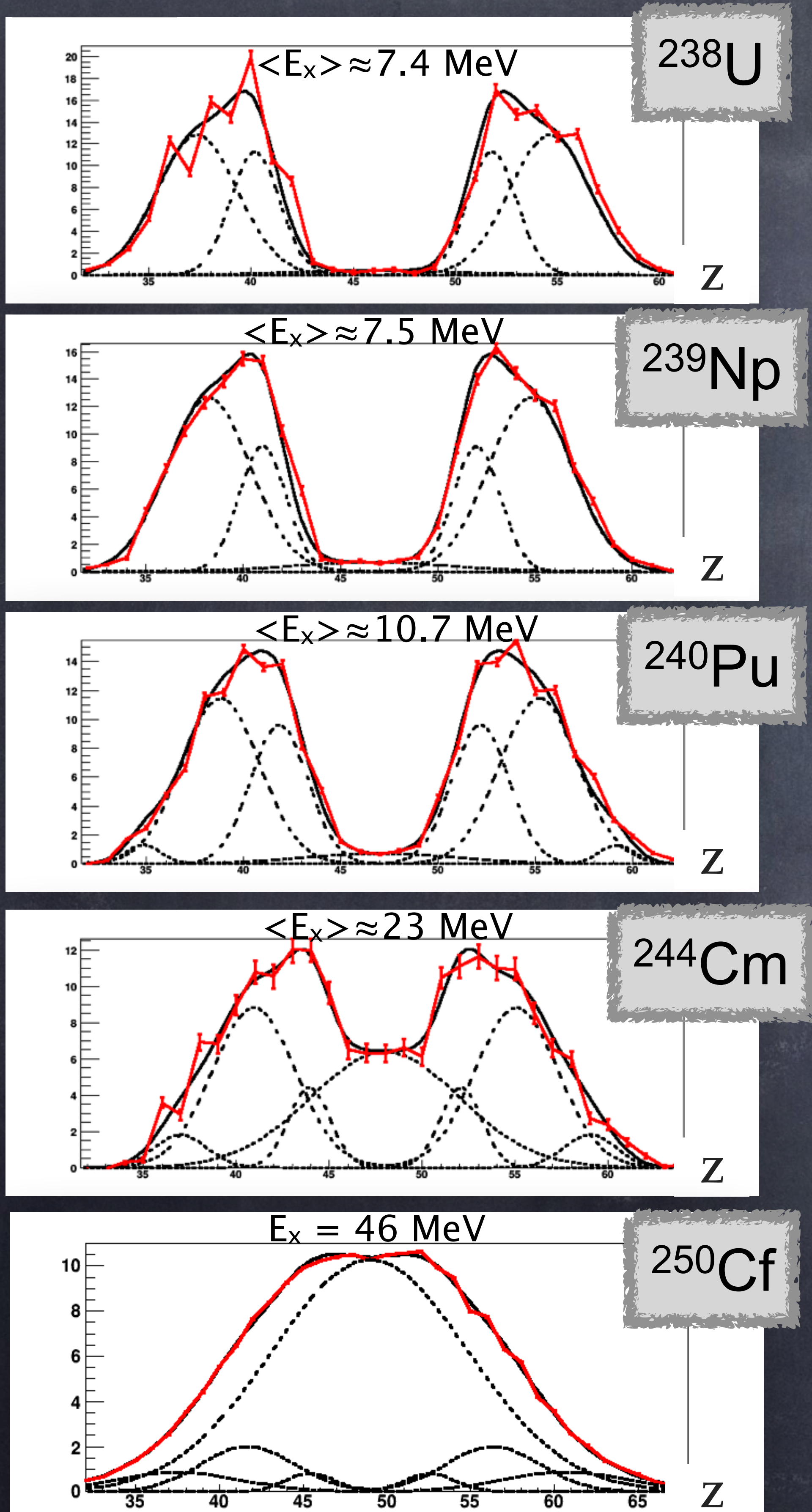

- Super Long (μ=Zfiss/2, σ =4)
- - Standard I
- - Standar II
- - Super Asymmetric

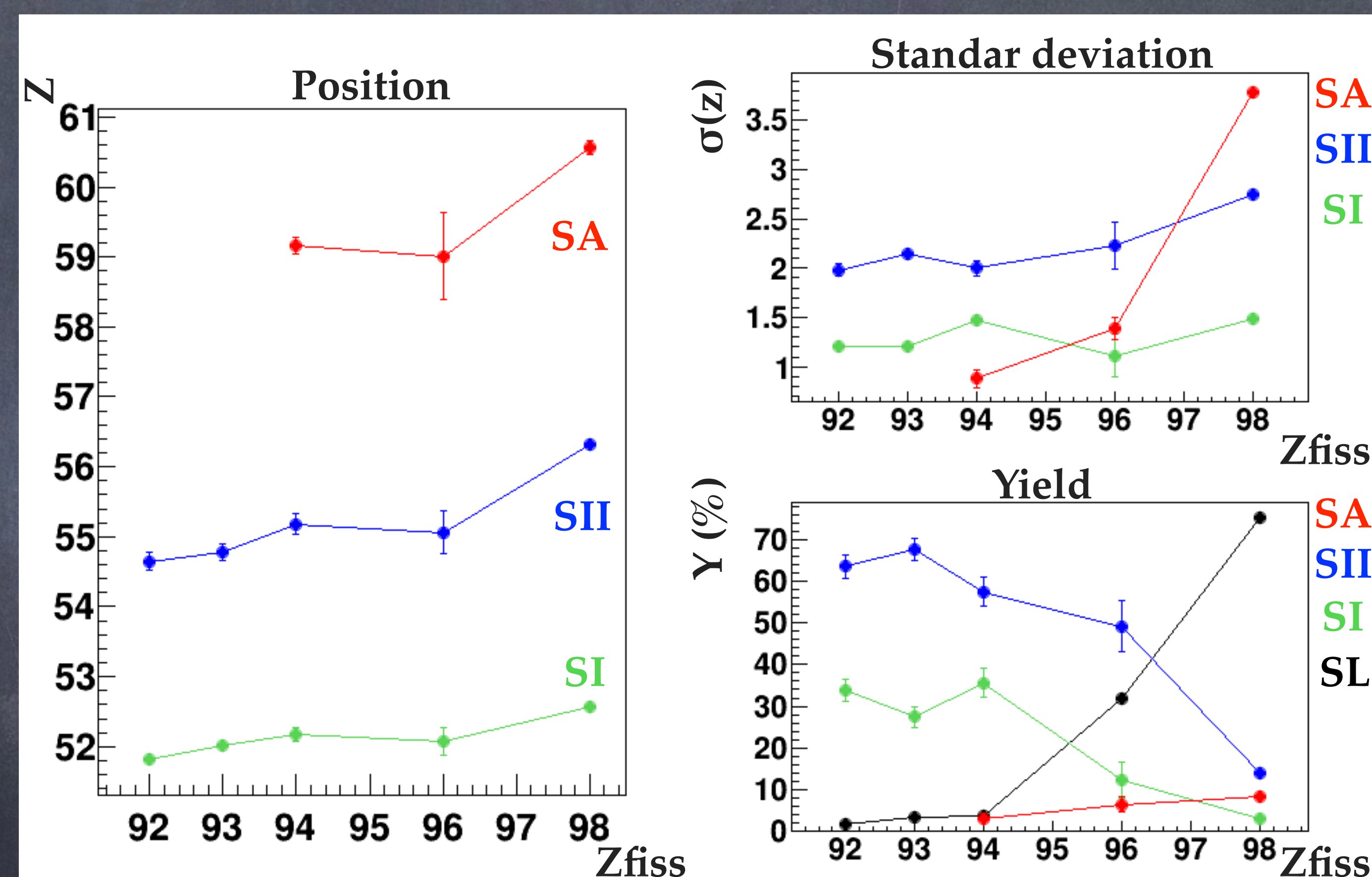

The position of the three modes presents a similar evolution with the fissioning system

SII is predominant in lighter fissioning system

Fission Modes

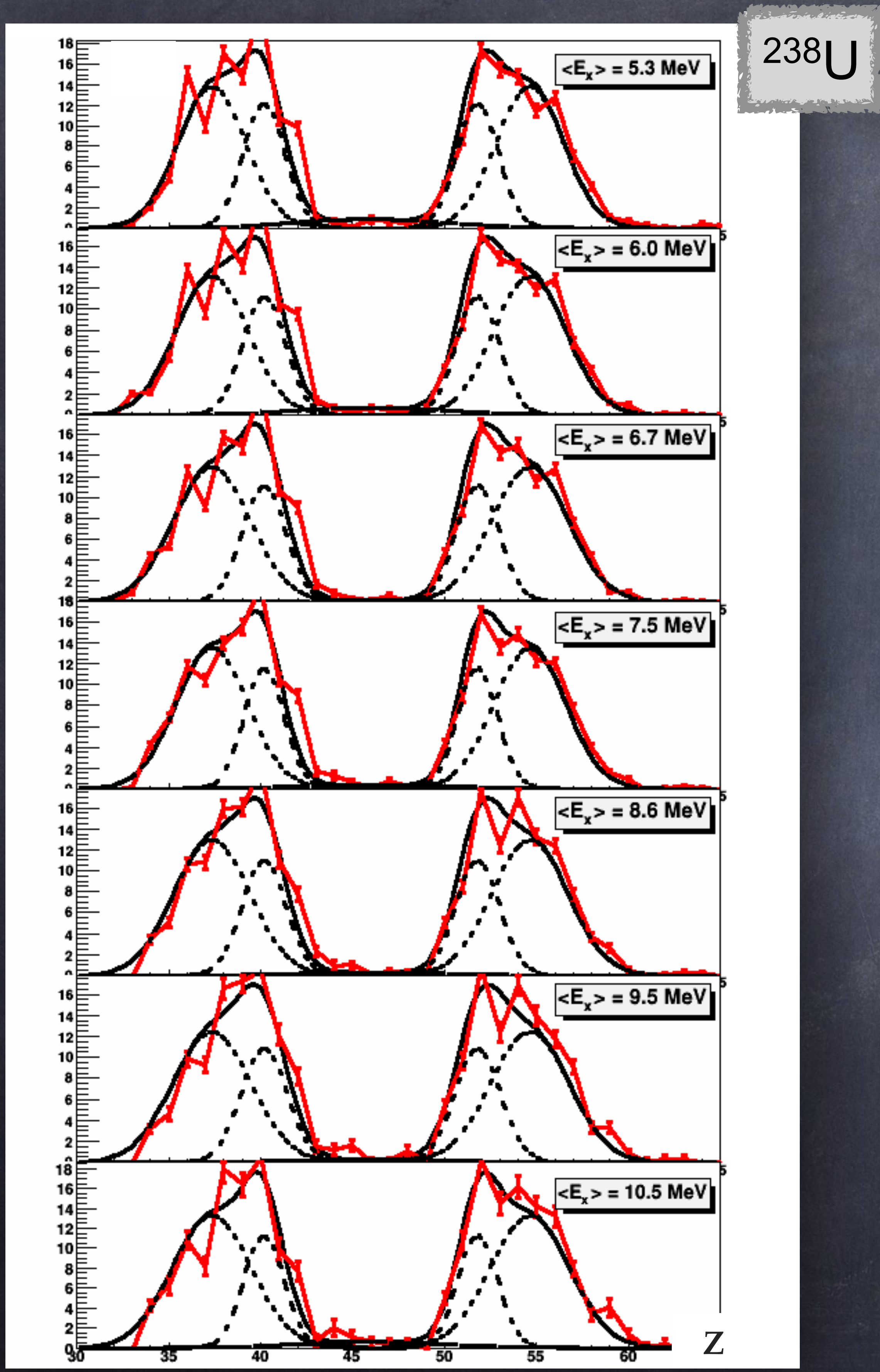

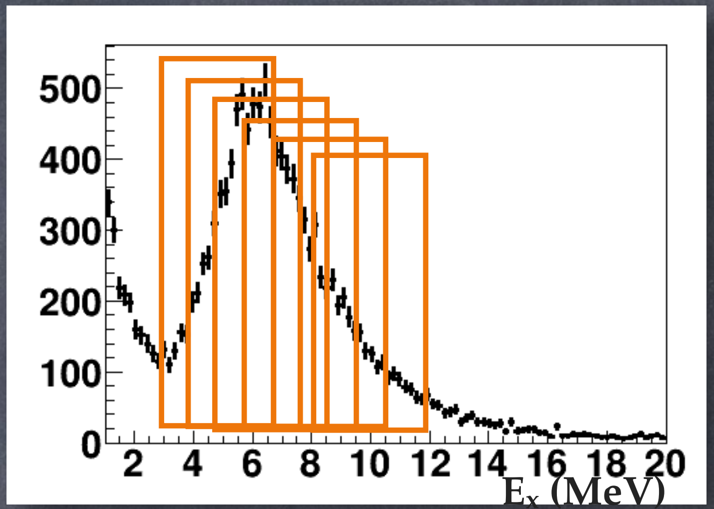

We study the fragment distributions for different positions of a gate moving along the E_x

Fission Modes positions fixed to the values obtained from the full Ex distribution fit

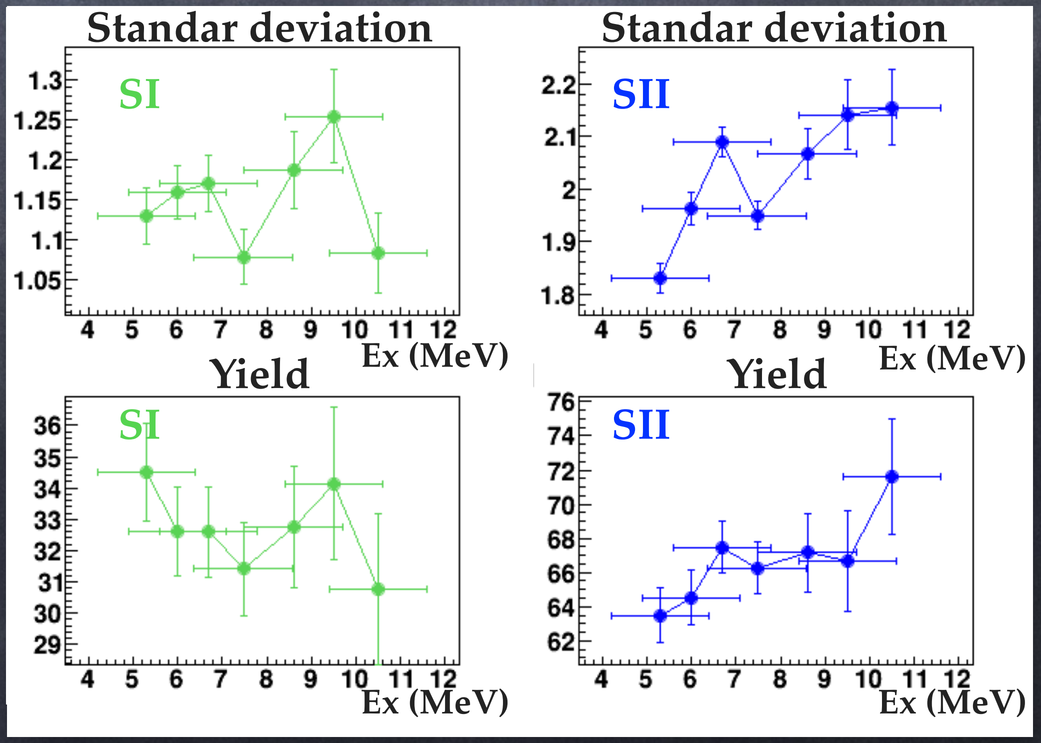

SII width increases with the excitation energy

Fission Modes

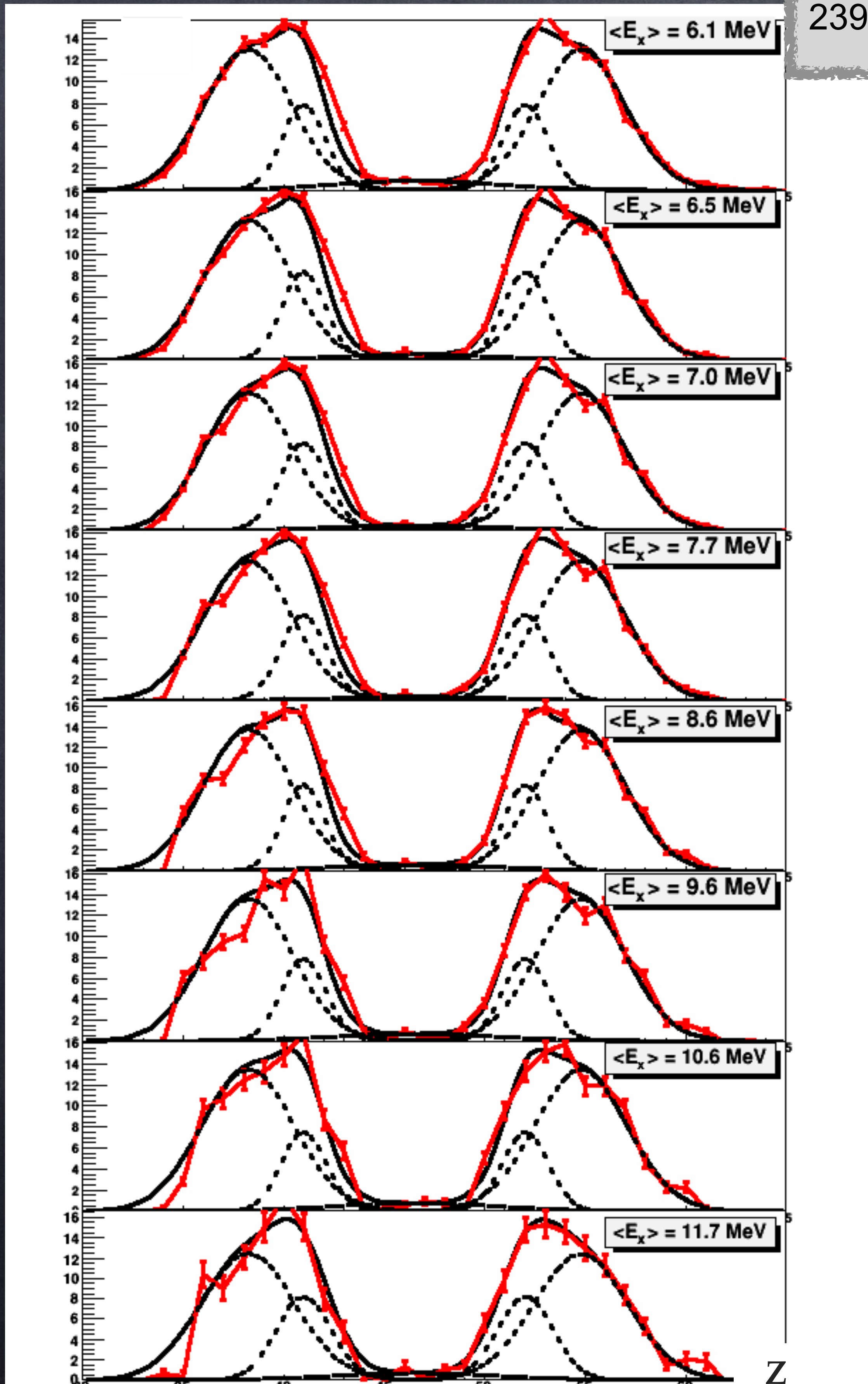

^{239}Np

SII width increases with the excitation energy

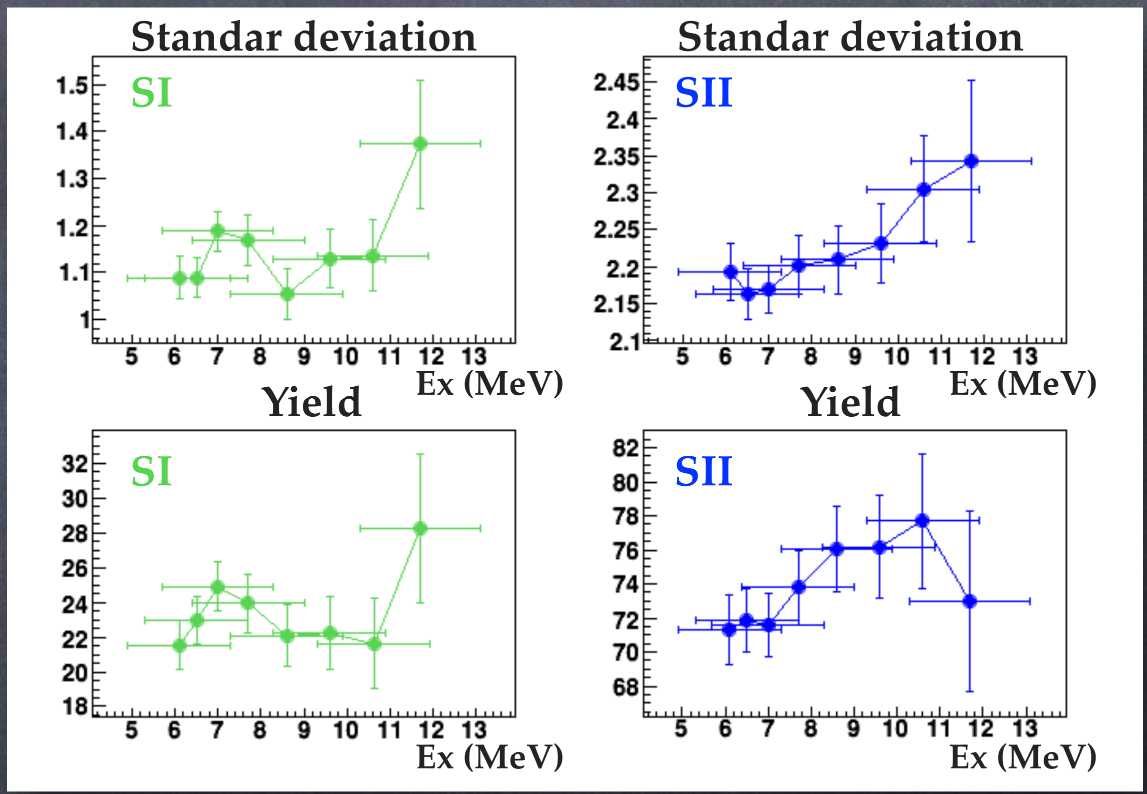

SII higher with higher Ex

Fission Modes

^{240}Pu

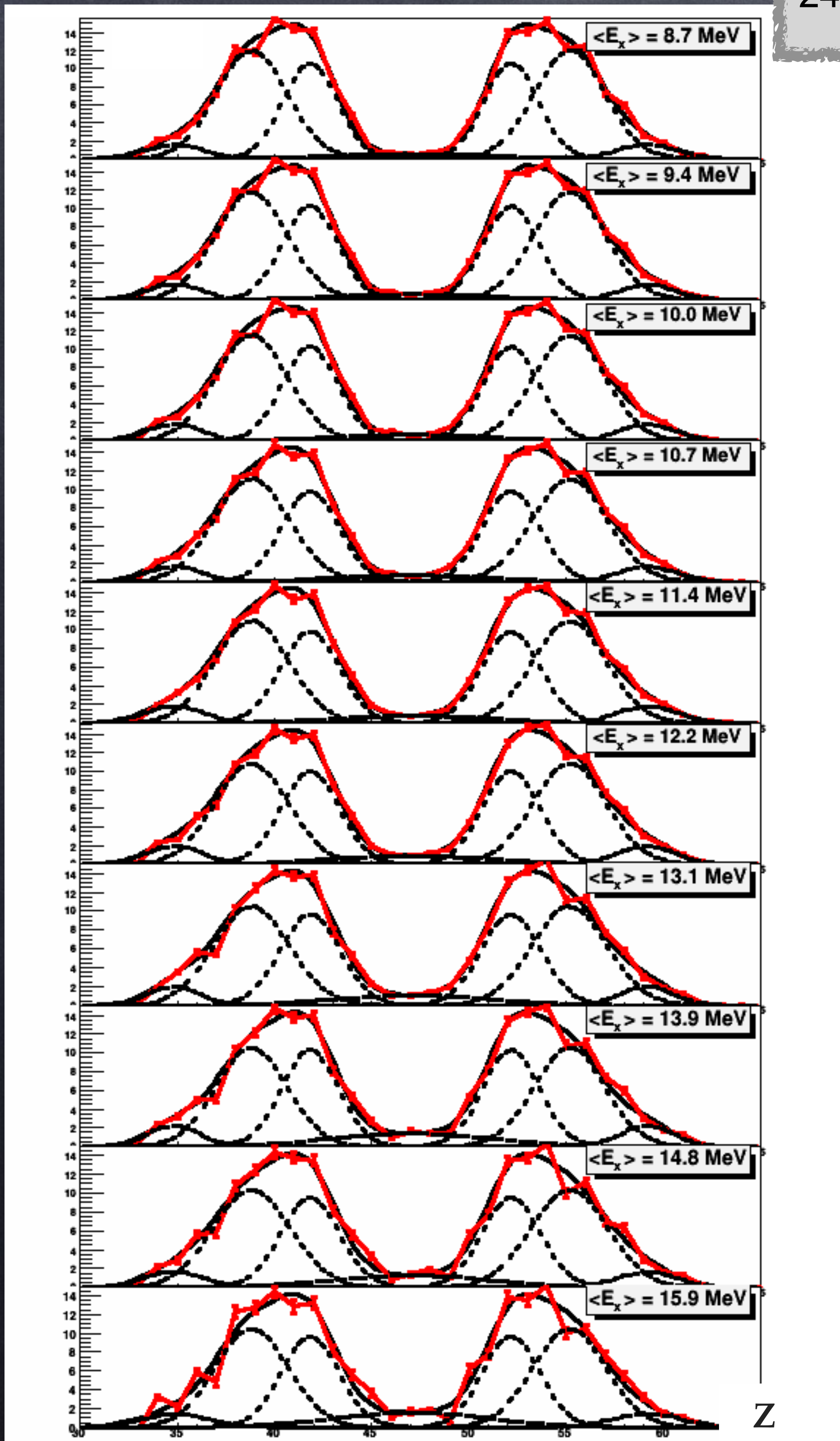

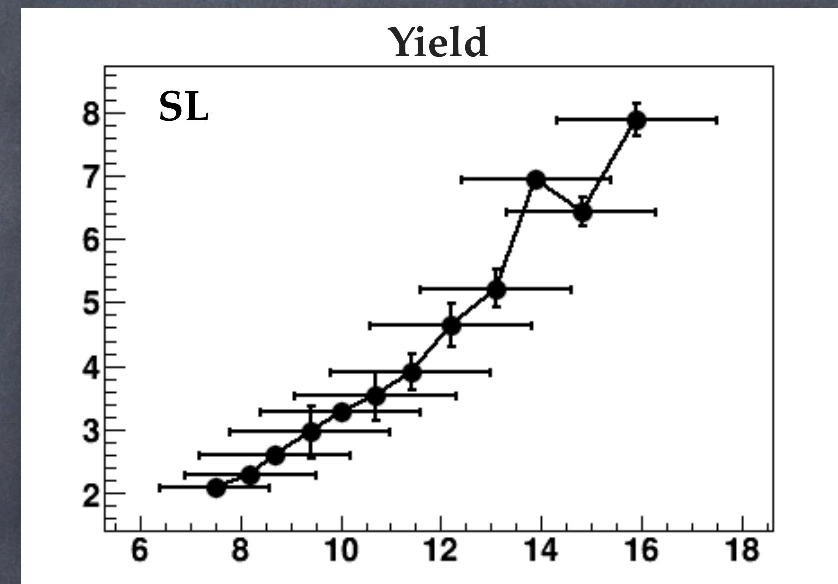

The yield of the Super Long mode increases with Ex

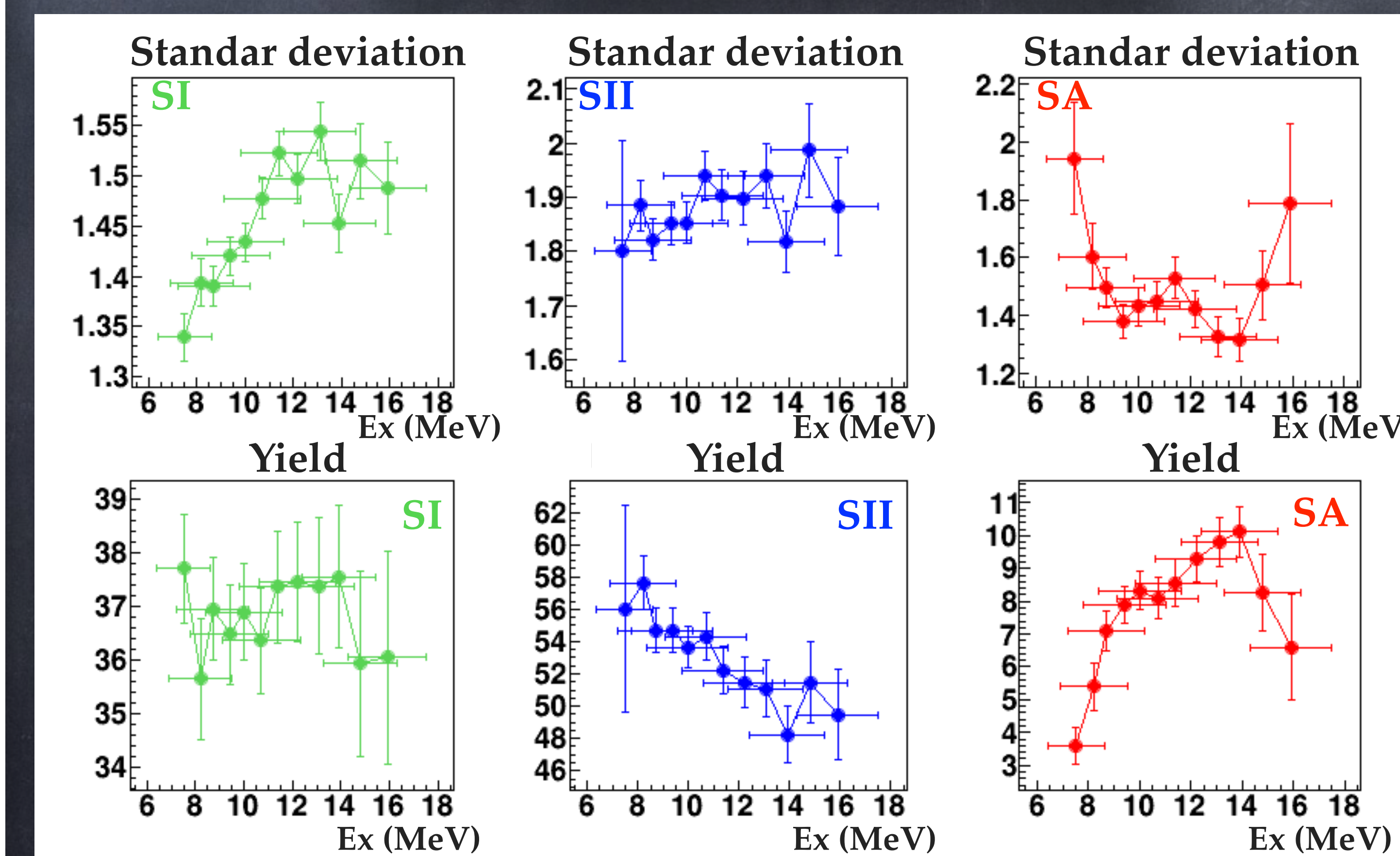

SII yield decreases with Ex competing with SL and SIII

Fission Modes

^{244}Cm

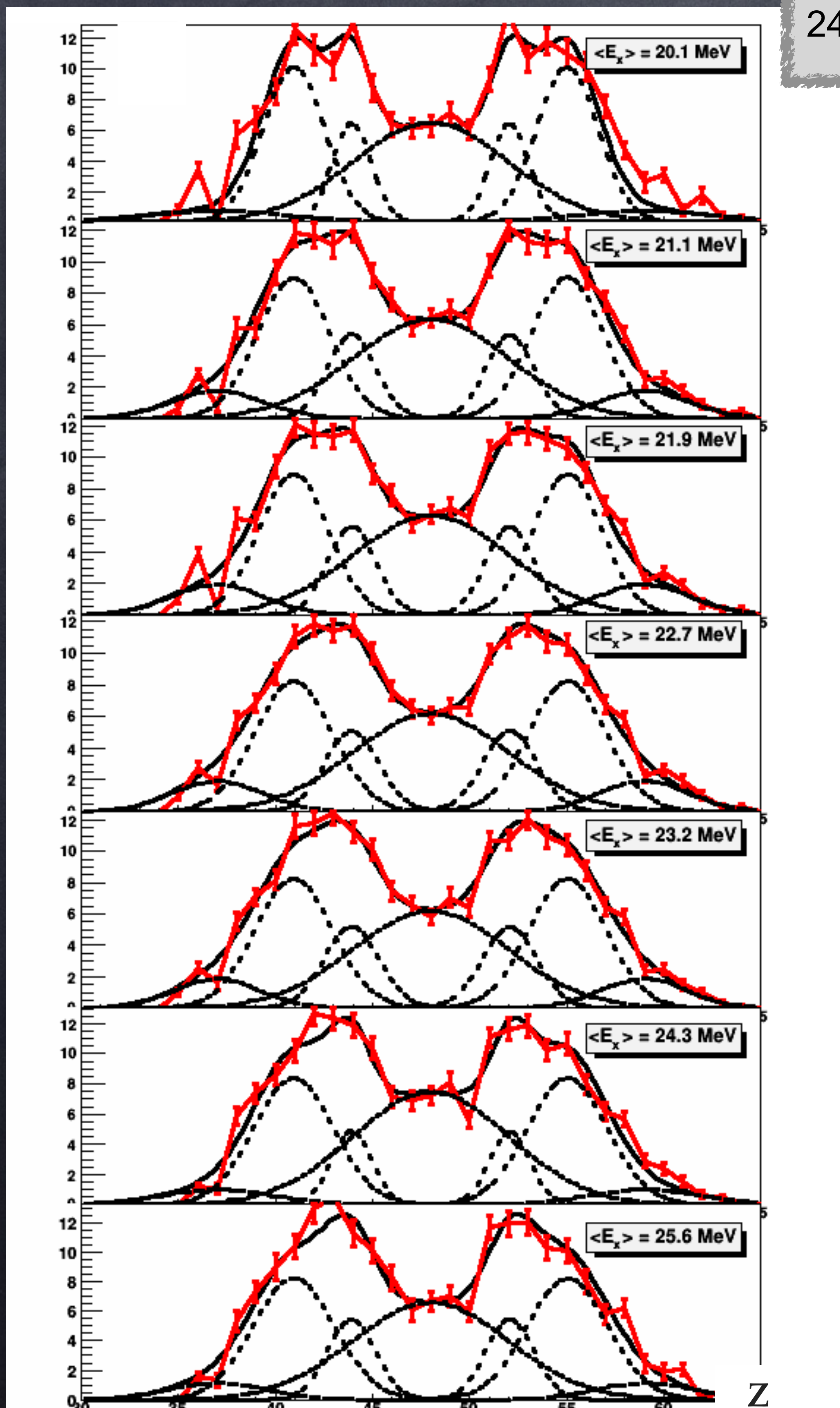

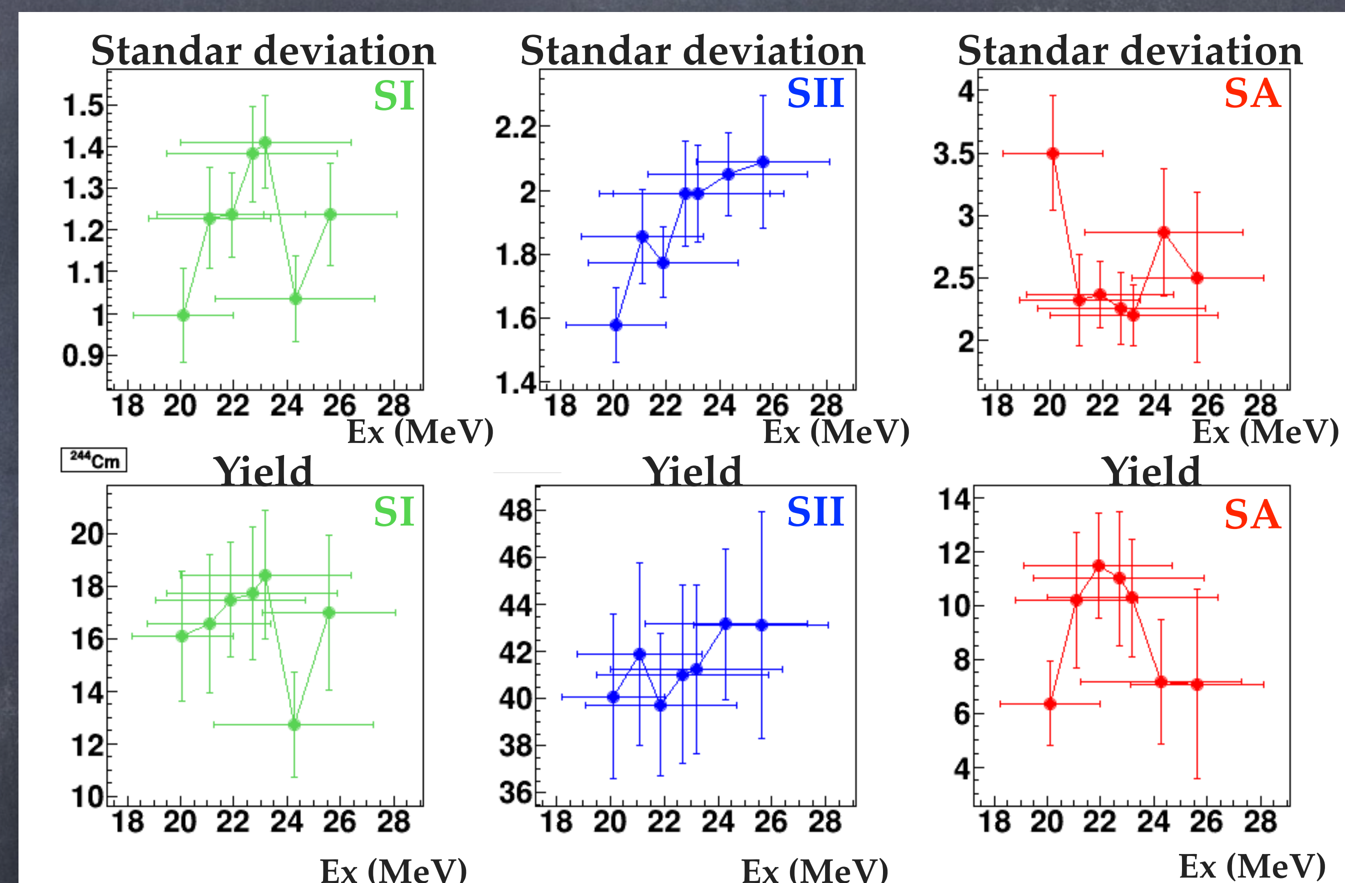

SII width increases with the excitation energy

Conclusions

The fission of 5 fissioning systems (^{238}U, ^{239}Np, ^{240}Pu, ^{244}Cm and ^{250}Cf), were investigated

Fissioning systems were produced by transfer reactions in inverse kinematics, and identified in SPIDER, allowing the measurement of their range of excitation energies

The VAMOS spectrometer permits the full isotopic identification of fission fragments

The determination of isotopic fission yields reveals structure effects, a larger charge polarization is present in lighter fissioning systems, where the neutron excess increases driven by the double magic nucleus ^{132}Sn

The structure effects were investigated as a function of the excitation energy, resulting in a reduction of the neutron excess, the asymmetric fission component, and the TKE, for higher Ex

The symmetric and two asymmetric modes (SL, SI, SII) were fitted to the fragments distribution of ^{238}U and ^{239}Np. A third asymmetric mode (SA) was need to describe ^{240}Pu, ^{244}Cm and ^{250}Cf cases

The position of the modes increases with the fissioning system, while the predominance of SII decreases

The fission modes were studied as a function of Ex, the SII mode presents a stronger dependence than SI or SA, with Ex. The SL-mode contribution is observed to increase with the Ex for ^{240}Pu